iScience

CellPress
OPEN ACCESS

Article

TIGIT contributes to the regulation of 4-1BB and does not define NK cell dysfunction in glioblastoma

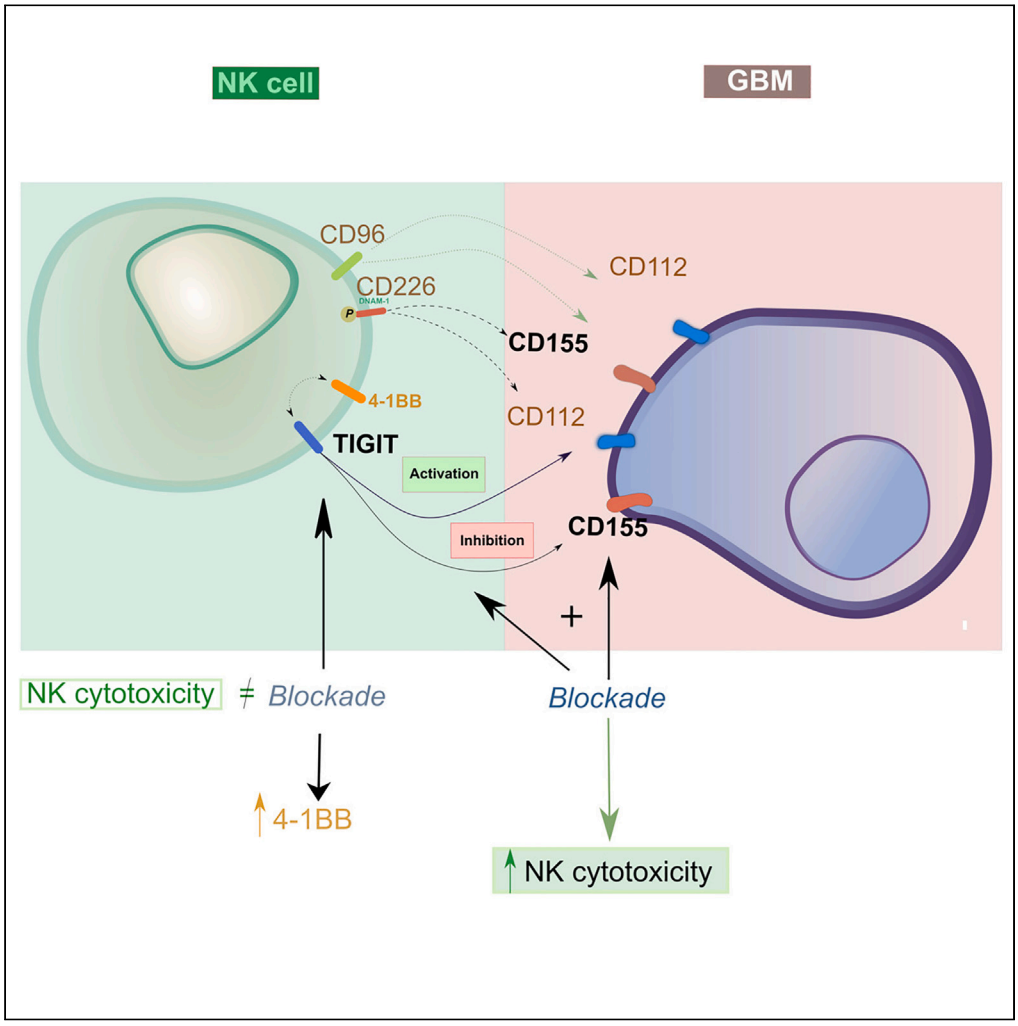

Kyle B. Lupo, Sandra Torregrosa-Allen, Bennett D. Elzey, ..., MacKenzie McIntosh, Karen E. Pollok, Sandro Matosevic

sandro@purdue.edu

Highlights

We report that TIGIT is not a marker of dysfunction on NK cells in GBM

TIGIT expression on NK cells correlates with that of 4-1BB

TIGIT^{+} NK cells are highly functional

TIGIT regulates heterogeneous responses on NK cells through multiple binding partners

Lupo et al., iScience *26*, 108353
December 15, 2023
https://doi.org/10.1016/j.isci.2023.108353

iScience

CellPress
OPEN ACCESS

Article

TIGIT contributes to the regulation of 4-1BB and does not define NK cell dysfunction in glioblastoma

Kyle B. Lupo,[1] Sandra Torregrosa-Allen,[2] Bennett D. Elzey,[2,3,4] Sagar Utturkar,[2] Nadia A. Lanman,[2,3] Aaron A. Cohen-Gadol,[5] Veronika Slivova,[6] MacKenzie McIntosh,[7] Karen E. Pollok,[8,9,10,11] and Sandro Matosevic[1,2,12,*]

SUMMARY

TIGIT is a receptor on human natural killer (NK) cells. Here, we report that TIGIT does not spontaneously induce inhibition of NK cells in glioblastoma (GBM), but rather acts as a decoy-like receptor, by usurping binding partners and regulating expression of NK activating ligands and receptors. Our data show that in GBM patients, one of the underpinnings of unresponsiveness to TIGIT blockade is that by targeting TIGIT, NK cells do not lose an inhibitory signal, but gains the potential for new interactions with other, shared, TIGIT ligands. Therefore, TIGIT does not define NK cell dysfunction in GBM. Further, in GBM, TIGIT$^+$ NK cells are hyperfunctional. In addition, we discovered that 4-1BB correlates with TIGIT expression, the agonism of which contributes to TIGIT immunotherapy. Overall, our data suggest that in GBM, TIGIT acts as a regulator of a complex network, and provide new clues about its use as an immunotherapeutic target.

INTRODUCTION

As immunotherapeutic effectors, NK cells are regulated by a combination of activating and inhibitory receptors which collectively drive the extent of their anti-tumor responses.[1] Interest in targeting these receptors in order to modulate the function of NK cells against solid tumors has motivated studies of the roles and mechanisms of receptor-ligand interactions in the context of NK cell-based immunotherapy.[2–4]

Among such receptors, TIGIT (T cell immunoglobulin and immunoreceptor tyrosine-based inhibitory motif domain) is expressed on both T and NK cells,[5] where it signals through its ITIM domains via two ligands, CD155 and CD112.[6] TIGIT has traditionally been considered a checkpoint receptor on NK cells, due to its ITIM signaling domain, and a marker of exhaustion and inhibition, upregulated on activated NK cells. Lack of responses to TIGIT blockade monotherapy have, however, challenged this notion but not provided clues about its functional role on NK cells. Though shown to induce inhibition of NK cells in a variety of cancers using both human and mouse models,[7–9] TIGIT is also associated with NK cell maturation and activation in mice.[10] This has muddled the initial perception of TIGIT as a purely inhibitory receptor and marker for NK cell dysfunction and opened the discussion for a more nuanced role of TIGIT in NK cell functional activation, supported by evidence that anti-TIGIT monotherapy has not been effective in enhancing CD8$^+$ T cell responses, controlling tumor growth in murine models or melanoma patient samples[11,12] or enhancing NK cell function[13] in human healthy donor and melanoma patient samples.

Where it was shown effective, TIGIT blockade was shown to rely on the presence and activity of NK cells as well as additional co-therapies for therapeutic efficacy, resulting in the reversal of NK cell exhaustion and promotion of anti-tumor effects in *in vivo* models of colon carcinoma, breast cancer and melanoma.[14] TIGIT expression was also upregulated in ovarian cancer patients,[15] while blockade of TIGIT augmented the effects of trastuzumab against breast cancer cells.[16] In soft tissue sarcoma, TIGIT was found to be upregulated on tumor-infiltrating NK (tiNK) cells, while stimulation with IL-15 enhanced the cytotoxicity of NK cells promoted by blockade of TIGIT.[17] Stimulation with IL-15 induced upregulation of TIGIT on NK cells, linking TIGIT with the cells' functional activation. The requirement of IL-15 stimulation for effectiveness of TIGIT blockade was described in a separate study, where blocking TIGIT resulted in the abrogation of *in vivo* melanoma tumor

[1]Department of Industrial and Physical Pharmacy, Purdue University, West Lafayette, IN, USA
[2]Center for Cancer Research, Purdue University, West Lafayette, IN, USA
[3]Department of Comparative Pathobiology, Purdue University, West Lafayette, IN, USA
[4]Department of Urology, Indiana University School of Medicine, Indianapolis, IN, USA
[5]Department of Neurological Surgery, Indiana University, Indianapolis, IN, USA
[6]Enterprise Clinical Research Operations Biorepository, Indiana University Health, Indianapolis, IN 46202, USA
[7]Histology Research Laboratory, Center for Comparative Translational Research, College of Veterinary Medicine, Purdue University, West Lafayette, IN, USA
[8]In Vivo Therapeutics Core, Indiana University Melvin and Bren Simon Comprehensive Cancer Center, Indiana University School of Medicine, Indianapolis, IN, USA
[9]Department of Pharmacology and Toxicology, Indiana University School of Medicine, Indianapolis, IN, USA
[10]Department of Pediatrics, Herman B Wells Center for Pediatric Research, Indiana University School of Medicine, Indianapolis, IN, USA
[11]Department of Medical and Molecular Genetics, Indiana University School of Medicine, Indianapolis, IN, USA
[12]Lead contact
*Correspondence: sandro@purdue.edu
https://doi.org/10.1016/j.isci.2023.108353

growth only in the presence of IL-15 stimulation.[13] Some studies have also shown that TIGIT$^+$ NK cells are less functional than TIGIT$^-$ cells against leukemia targets, though these assays did not use sorted NK cells.[18]

The contribution of TIGIT to NK cell activation is not a new concept: TIGIT was shown to be a marker for NK cell activation in healthy individuals,[19] and TIGIT$^+$ NK cells isolated from melanoma tumors correlated with upregulation of activation and effector markers.[13] In line with these observations and in contrast to other findings made in solid tumors, NK cells from acute myeloid leukemia (AML) patients downregulated TIGIT compared to healthy individuals, while AML patient-derived TIGIT$^+$ NK cells showed enhanced cytotoxicity, cytokine production and Granzyme B expression.[20] Other studies in AML pointed out that allogeneic stem cell transplantation (alloSCT) recipients with higher TIGIT expression had lower NK cell counts in the bone marrow, but unchanged T cell counts.[21]

The inhibitory functions of TIGIT rely largely on CD155 (PVR) due to high binding affinity between these two receptors (6, 22), a regulator of a complex network of interactions with NK cells which includes stimulation of NK cell activity via CD226, another ligand for CD155 and an activating NK cell receptor. To add to the complexity of this axis, CD155 also interacts with CD96, an NK cell receptor that has been reported to have both activating and inhibitory function.[22] This axis was recently shown to regulate NK cell cytotoxicity in melanoma.[23]

We sought to understand the role of TIGIT on NK cells and the clues underlying its unresponsiveness to checkpoint blockade. Here, we report our findings that TIGIT behaves as a decoy-like receptor, regulating a complex network in glioblastoma (GBM). It does so by associating with mature and cytotoxic NK cells. In addition, TIGIT downregulates activating receptors rather than itself induces inhibition. Despite its capacity for NK cell inhibition due to its ITIM domains, TIGIT does not promote inhibitory signaling in GBM, nor is it a marker of NK cell exhaustion. Phenotypic screens and functional assays of changes in NK cell activating receptors revealed 4-1BB, more than other NK cell receptors, to correlate with TIGIT expression. 4-1BB, member of the TNFR superfamily, is a co-stimulatory molecule expressed on primed NK cells with roles in the support of NK cell activity,[24] with the ability to induce NK cell activation upon its agonism.[25] In our study, responses to TIGIT blockade on NK cells further correlated with enhanced expression of 4-1BB over other receptors in supporting NK cell effector function. While TIGIT$^+$ NK cells are more functional against cancer targets, their anti-tumor responses correlate with expression of 4-1BB and activity of CD155. However, despite strong expression relationships with TIGIT in patient and healthy adult data, 4-1BB modulation is not by itself sufficient to dominate responses to TIGIT modulation, likely acting in concert with other TIGIT co-receptors and signaling partners. Nonetheless, the involvement of 4-1BB in TIGIT signaling is a new interaction, not previously described that might be utilized in effective TIGIT immunotherapy. These data provide important clues as to the reasons underlying failure of TIGIT blockade monotherapy in GBM, and highlight the need to consider the broader molecular landscape of of the TIGIT signaling network.

RESULTS

Exhaustion markers PD-1 and LAG-3, but not TIGIT, are upregulated in GBM

The NK cell surface receptor TIGIT has been reported to induce immunosuppression when binding with the inhibitory ligands, CD155 or CD112, on GBM, although with a weaker affinity for CD112.[26] CD155 and CD112 also bind to inhibitory receptor CD96 and activating receptor DNAM-1 (Figure 1A) on NK cells, contributing to a large network balancing activating and inhibitory NK cell responses. However, the mechanism driving TIGIT-induced responses is not well characterized, nor is the relationship between TIGIT and other NK cell receptors, such as PD-1, LAG-3, CD69, and 4-1BB (Figure 1A). Kaplan-Meier survival plots for GBM based on The Cancer Genome Atlans Program (TCGA) data show a negative prognostic role of TIGIT and CD155 in GBM patients, as well as a negative prognostic role of TIGIT and CD112 in GBM patients (Figures 1B and S4). Similary, CD155 expression negatively correlates with NK cell and CD8 T cell infiltration into GBM tumors, with high CD155 expression and high NK cell infiltration corresponding to better overall survival (Figures S5 and S6). While co-expression of CD155 and TIGIT acted as negative prognostic factors in GBM, expression of either TIGIT alone or CD155 alone did not show significance in overall patient survival.

To establish the identity of tumor infiltrating (tiNK) and circulating (cNK) cells in GBM patients, we assessed the phenotypic differences between NK cells collected from healthy donors, and cNK and tiNK cells collected from GBM patients via flow cytometry. tiNK cells were characterized by significantly higher levels of 4-1BB, PD-1 and LAG-3 than cNK cells from GBM patients and healthy donors, as well as significantly lower levels of CD94 and CD69 (Figures 1C–1E and S1). Further, CD57 was upregulated on tiNK cells compared to cNK cells from GBM patients and healthy donors (Figures 1C–1E and S1), while no significant differences in TIGIT expression were observed between tiNK or cNK from GBM patients and healthy donors, suggesting that TIGIT may not be an NK cell exhaustion marker, such as PD-1 or LAG-3, in the context of GBM. 4-1BB also showed among the highest correlation coefficients with the expression of TIGIT and both circulating and tumor-infiltrating NK cells (Figure S7). Additionally, TIGIT expression on cNK cells as well as tiNK cells from GBM patients correlated with 4-1BB expression with an R^2 value of 0.7738 and 0.8416, respectively, suggesting for the first time a coexpression, and potential relationship between TIGIT and 4-1BB on NK cells in GBM (Figure 1F, 1G, and S7). In terms of NK cell frequency, no correlation between TIGIT and 4-1BB percentage was observed on cNK cells from patients, and only a weak correlation ($R^2 > 0.25$) on tiNKs was observed.

TIGIT expressing NK cells exhibit enhanced activation and maturity genotype over TIGIT$^-$ NK cells

To investigate the role of TIGIT in NK cell activation and exhaustion, we performed RNA-seq analysis on human TIGIT^{high}, TIGIT^{medium}, and TIGIT^{negative} NK cells. RNA extracted from human NK cells from healthy donors sorted based on TIGIT expression (TIGIT^{high}, TIGIT^{medium}, TIGIT^{negative}) was sequenced. TIGIT^{high} and TIGIT^{medium} NK cell groups were both TIGIT$^+$, with protein expression levels above isotype control, and TIGIT^{negative} NK cells served as a negative control with protein expression levels below isotype control. The overall mapping rate was >90% for all samples. We identified differences between TIGIT^{high} and TIGIT^{negative} NK cells, as well as TIGIT^{medium} and TIGIT^{negative} NK cells

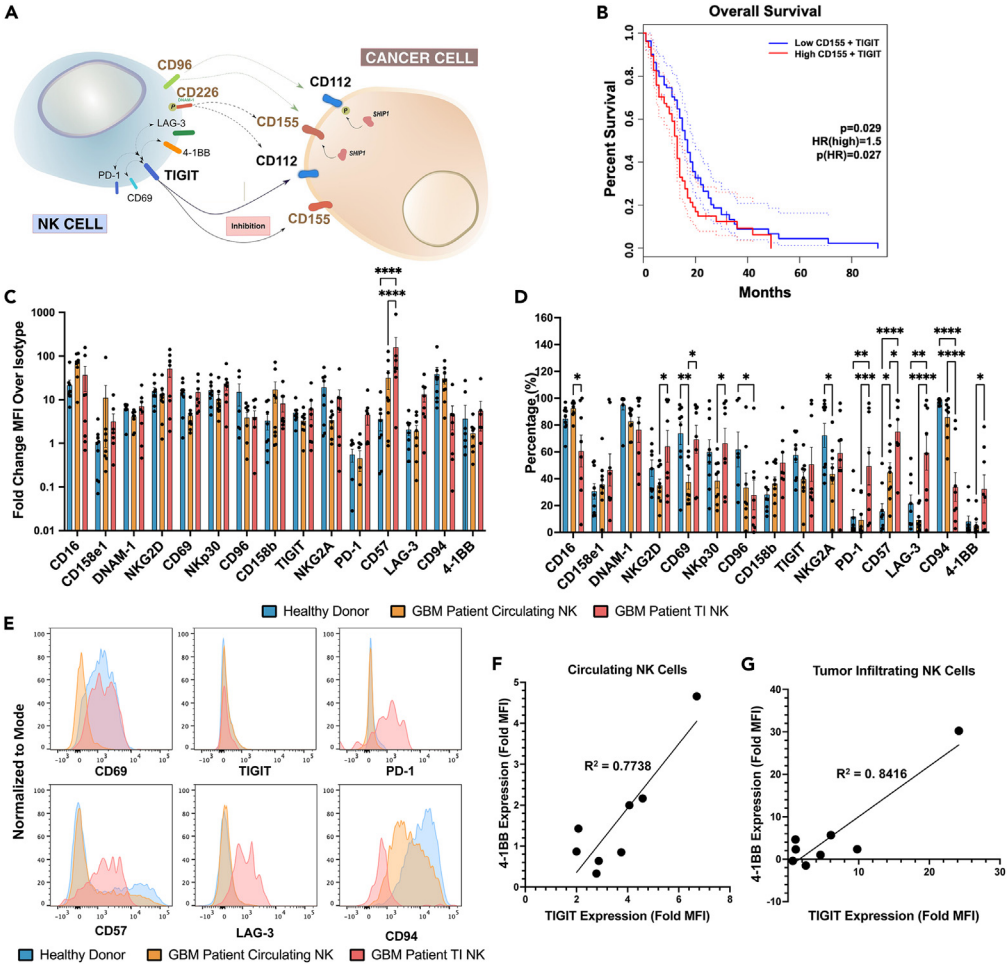

Figure 1. Exhaustion markers PD-1 and LAG-3 are upregulated in GBM patients, but not TIGIT

(A) Diagram depicting interactions between TIGIT, DNAM-1, CD96 and CD155, CD112, as well as intracellular cross-talk between TIGIT and other NK cell receptors (PD-1, 4-1BB, CD69, LAG-3.

(B) TCGA Kaplan-Meier survival plot indicating that, together, CD155 and TIGIT are prognostic factors in GBM. High CD155 + TIGIT = 81 patients; Low CD155 + TIGIT = 81 patients.

(C and D) Groups were compared by Kaplan-Meier survival analysis. Bar plots depicting (C) MFI (*left*) and (D) percentage (*right*) expression of NK cell activating (CD16, DNAM-1, NKG2D, CD69, NKp30, CD57, 4-1BB) and inhibitory (CD158e1, CD96, CD158b, TIGIT, NKG2A, PD-1, LAG-3, CD94) receptors on GBM patient cNK and tiNK cells, as well as NK cells from healthy donors (n = *8 patients*). Groups were compared using ordinary one-way ANOVA and Tukey's post-hoc test.

(E) Histograms depicting differences in select NK ligands between healthy donors, GBM patient cNK, and GBM patient tiNK cells.

(F and G) Correlation between TIGIT expression (Fold MFI) and 4-1BB expression (Fold MFI) on (F) cNK (R^2 = 0.9181) and (G) tiNK (R^2 = 0.9649) cells harvested from GBM patients (n = 6). R^2 was calculated by simple linear regression. *p < *0.05*, **p < *0.01*, ***p < *0.001*, ****p < *0.0001*.

through differential gene expression analysis using DESeq2 and EdgeR software with a False Discovery Rate (FDR) threshold of <0.01. We identified 5,975 differentially expressed genes in TIGIT^{high} NK cells and 1,273 differentially expressed genes in TIGIT^{medium} NK cells, using TIGIT^{negative} NK cells as a control, with 1,244 differentially expressed genes shared between these two groups (Figures S8A and S8B). Of these genes, we identified 111 NK-specific genes with 67 differentially expressed only in TIGIT^{high}, 44 differentially expressed in TIGIT^{high} and TIGIT^{medium}, and 0 differentially expressed only in TIGIT^{medium} (Figures 2A, S8B, and S8C; Table S1). Further, principal component analysis revealed distinct differences between TIGIT^{high}, TIGIT^{medium}, and TIGIT^{negative} NK cells (Figure S8C). We categorized these 111 genes into groups based on their functional relation to NK cell status (activation, inhibition, maturation, migration, and other). Our analysis showed that TIGIT^{high} NK cells have a higher percentage of activation and maturation genes that were upregulated (TIGIT^{high}: 55.81% and 23.26%; TIGIT^{medium}: 69.23% and 7.69%) than downregulated (TIGIT^{high}: 36.11% and 13.89%; TIGIT^{low}: 0.00% and 50.00%), congruent with our observation that TIGIT expression correlated with enhanced NK cell functions (Figures 2A–2D). Specifically, *IL2RA* and *TNFRSF9* (4-1BB) were significantly upregulated on TIGIT^{+} (TIGIT^{high} and TIGIT^{medium}) over TIGIT^{negative} NK cells, suggesting the level of TIGIT expression may indicate NK cell activation and confirming the correlation between 4-1BB and TIGIT phenotype and function (Figure 2A). Further, *CXCR4*

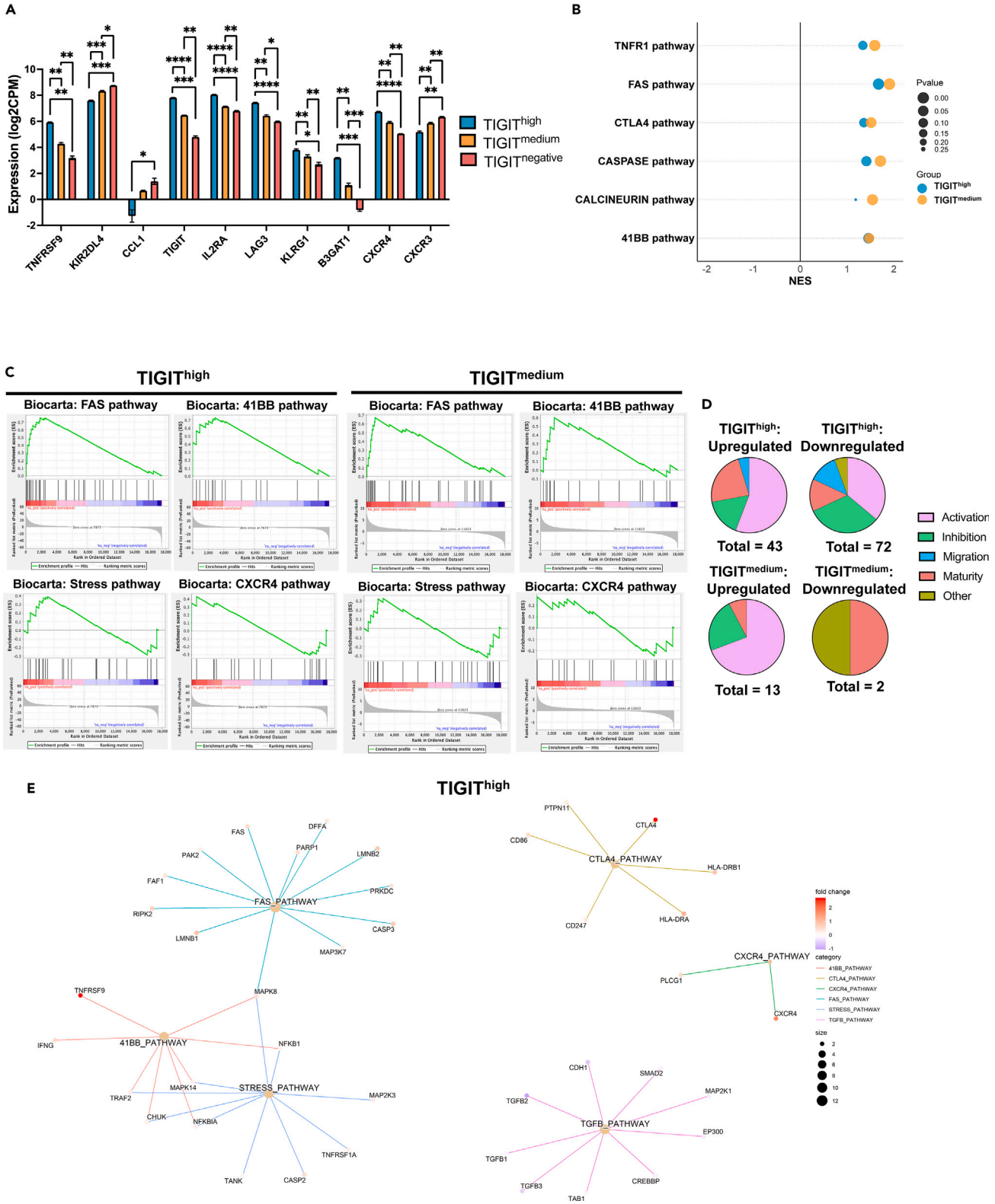

Figure 2. TIGIT^{high} NK cells exhibit enhanced activation and maturity genotype over TIGIT^{negative} NK cells

(A) Differential expression (log2CPM) of select NK cell genes related to maturity and activation TIGIT^{high}, TIGIT^{medium}, and TIGIT^{negative} NK cells (n = 3). Groups were compared using ordinary one-way ANOVA and Tukey's post-hoc test.

Figure 2. *Continued*

(B) Bubble chart of GSEA analysis NES and p value scores for select NK-relevant gene set from the Biocarta database.

(C) Running enrichment score (ES) analysis of FAS, 4-1BB, Stress, and CXCR4 pathways for sorted TIGIT^{high} (*left*) and TIGIT^{medium} (*right*) NK cells.

(D) Relative proportion of activation, inhibition, maturation, migration, and other NK genes up- and downregulated on sorted TIGIT^{high} (*left*) and TIGIT^{medium} (*right*) NK cells.

(E) ClusterProfiler map of differentially expressed genes in for TIGIT^{high} NK cells FAS, 4-1BB, Stress, CXCR4, CTLA-4, and TGF-B pathways. Data are represented as mean ± SEM. *p < *0.05*, **p < *0.01*, ***p < *0.001*, ****p < *0.0001*.

and *B3GAT1* (CD57) were upregulated, while *CXCR3* was downregulated, on TIGIT^{+} NK cells, indicating that TIGIT^{+} NK cells may have enhanced maturity. Additionally, *LAG-3* and *KLRG1* were upregulated and *KIR2DL4* was downregulated on all TIGIT^{+} NK cells, while *CCL1* was downregulated on only TIGIT^{high} NK cells.

Gene set enrichment analysis (GSEA) using the Biocarta gene database revealed that a number of pathways were significantly enriched (positive NES) in either TIGIT^{high}, TIGIT^{medium}, or both over TIGIT^{negative} NK cells. Namely, the FAS pathway was significantly enriched in TIGIT^{high} and TIGIT^{medium} ($p < 0.05$), while the 4-1BB pathway was significantly enriched in TIGIT^{high} but not TIGIT^{medium}, indicating a positive correlation between TIGIT expression and NK cell activation, and providing further evidence of a correlation between TIGIT and 4-1BB on NK cells (Figures 2B, 2C, and S9; Tables S2 and S3). TNFR1, CTLA4, CASPASE, and CALCINEURIN were all significantly enriched in TIGIT^{medium} but not TIGIT^{high}. Further, we mapped genes involved in the 4-1BB and FAS pathways, along with other NK cell relevant pathways (STRESS, CTLA4, TGFB, and CXCR4) with clusterProfiler and found many of the previously identified differentially expressed NK cell genes represented in these pathways of interest, including *TNFRSF9*, *CTLA4*, *FAS* and *TGFB1*. (Figures 2E and S9B).

Human TIGIT^{high} NK cells are more functional and overexpress activating receptors

Stimulated by the apparent involvement of 4-1BB in TIGIT activation and the lack of responses to TIGIT blockade monotherapy, as well as a genetic profile suggesting TIGIT expression correlates with functional maturity of NK cells, we explored the function and role of TIGIT on human NK cells. NK cells collected from the peripheral blood of healthy donors were first analyzed for expression of a panel of NK cell activating (CD16, CD69, DNAM-1, NKG2D, NKp30, CD96, NKp46, 4-1BB) and inhibitory (A2AR, CD158b, CD158e1, TIGIT, CD57 NKG2A/CD94, LAG-3, PD-1, TIM-3) receptors. CD56^{+}CD3^{-} NK cells were gated according to expression of TIGIT (TIGIT^{high}, TIGIT^{medium}, and TIGIT^{negative}). TIGIT^{high} NK cells presented with a more active NK cell phenotype, with significantly higher levels of CD16, CD69, NKG2D, and 4-1BB than TIGIT^{negative} NK cells (Figures 3A, S1–S3, and S10). TIGIT^{high} NK cells also had higher levels of PD-1 and TIM-3 than TIGIT^{negative} NK cells, but no significant differences in inhibitory KIRs (CD158b, CD158e1) or NKG2A/CD94 were observed. This phenotype suggested that TIGIT^{high} NK cells appear to be more active and potentially more functional than TIGIT^{negative} NK cells.

To test this hypothesis, we sorted these NK cells based on expression of TIGIT, and compared NK cell functionality between these subpopulations. TIGIT^{high} NK cells were able to lyse GBM43 target cells at significantly higher levels than either TIGIT^{medium} or TIGIT^{negative} NK cells (Figure 3B). In addition, TIGIT^{high} NK cells also exhibited higher levels of degranulation, measured via CD107a expression in each donor tested, and significantly higher levels of IFN-γ secretion in all but one donor (Figures 3C–3E and S11). TIGIT^{high} NK cells also exhibited significantly higher levels of glycolysis than TIGIT^{medium} or TIGIT^{negative} NK cells, indicative of a more metabolically-active cell type (Figures 3E–3F). Altogether, TIGIT-expressing NK cells exhibit enhanced functionality over TIGIT^{negative} NK cells, suggesting that TIGIT expression on peripheral blood-derived NK cells may not be indicative of NK cell exhaustion, but may mark functionally-competent NK cells.

TIGIT blockade correlates with low CD16, high 4-1BB, and higher inflammatory cytokines

To understand the impact of CD155 and TIGIT signaling on NK cell function, we blocked these two ligands, either independently or together, and measured the expression of a panel of NK cell activating (CD16, 4-1BB, DNAM-1, NKG2D, CD69, NKp30) and inhibitory (LAG-3, CD158e1, CD158b, A2AR, PD-1, CD57, TIM-3, NKG2A/CD94, KLRG-1) receptors via flow cytometry (Figures 4A–4E, S1, and S12). When challenged with a primary patient-derived GBM cell line (GBM43) over 24 h in the presence of a blocking anti-TIGIT mAb, NK cells showed significant downregulation of CD16 and significant upregulation of 4-1BB. This was true both in the presence or absence of anti-CD155 blockade (Figures 4B and 4C). LAG-3 expression showed significant upregulation in the presence of anti-TIGIT blockade alone, but not with dual anti-TIGIT/CD155 blockade (Figure 4D). Further, we did not detect any soluble CD16 in the supernatant, suggesting the decrease in CD16 expression is induced by downregulation, and not shedding of CD16 (Figure S13).

Following co-culture with GBM cells, cell supernatants were collected and a multiplex array of a panel of pro-inflammatory cytokines was measured (Figures 4F and 4G). TIGIT blockade alone induced significant upregulation in the secretion of TNF-α as well as IL-1β (Figures 4F and 4G), while CD155 blockade alone induced significant downregulation of secreted IFN-γ, IL-5, TNF-α, IL-10, and GM-CSF (Figures 4F and 4G). Altogether, this suggested that targeting of TIGIT alone is able to enhance NK cell activation, though this activation does not translate to enhanced cytotoxicity, further indicating that TIGIT's inhibitory role may not be directly through inhibitory signaling, but rather through interactions with other NK cell receptors, such as CD16, 4-1BB, and others. To corroborate observations on upregulation of 4-1BB on NK cells upon blockade of TIGIT, we generated CRISPR/Cas9 TIGIT^{KO} human NK cells. When challenged to kill GBM43 cells, loss of TIGIT on NK cells correlated to a significant upregulation of 4-1BB expression, validating the co-expression relationship between TIGIT and 4-1BB observed upon TIGIT blockade (Figures 4H and S14).

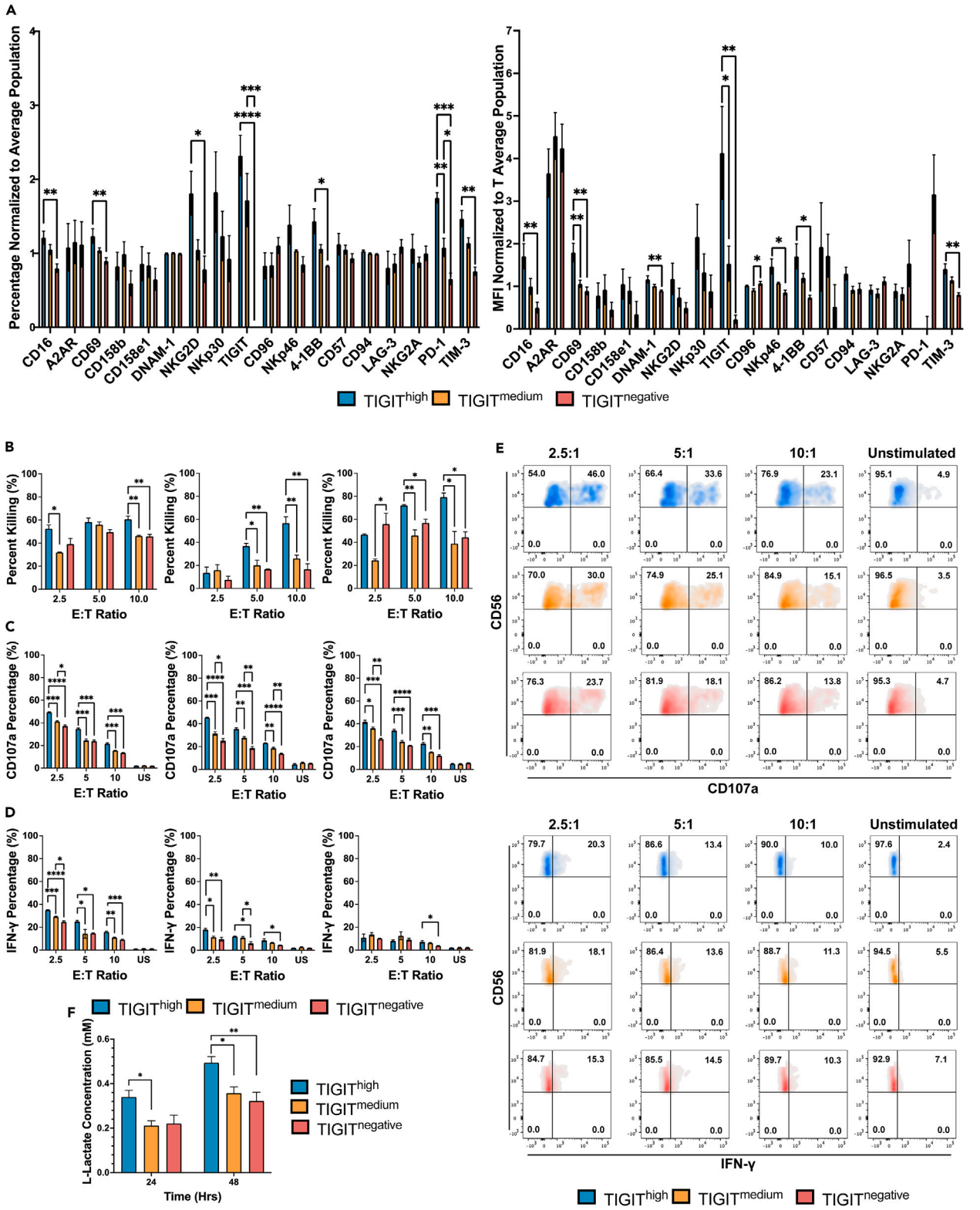

Figure 3. TIGIT^{high} NK cells are more functional and overexpress activating receptors

(A) Normalized percentage (*left*) and MFI (right) expression of NK cell receptors on sorted TIGIT^{high}, TIGIT^{medium}, and TIGIT^{negative} NK cells and (*below*) representative flow cytometric gating strategy for sorting these NK cell subsets (n = 3). Groups were compared using ordinary one-way ANOVA and Tukey's post-hoc test.

Figure 3. *Continued*

(B) Cytolysis of GBM43-WT cells by sorted TIGIT^{high}, TIGIT^{medium}, and TIGIT^{negative} NK cells at E:T ratios 2.5:1, 5:1, and 10:1 (n = 3). Groups were compared using ordinary one-way ANOVA and Tukey's post-hoc test.

(C) CD107a expression in response to GBM43-WT cells by sorted TIGIT^{high}, TIGIT^{medium}, and TIGIT^{negative} NK cells at E:T ratios 2.5:1, 5:1, and 10:1 (n = 3). Groups were compared using ordinary one-way ANOVA and Tukey's post-hoc test.

(D) IFN-γ expression in response to GBM43-WT cells by sorted TIGIT^{high}, TIGIT^{medium}, and TIGIT^{negative} NK cells at E:T ratios 2.5:1, 5:1, and 10:1 (n = 3). Data are shown for each individual donor. Groups were compared using ordinary one-way ANOVA and Tukey's post-hoc test.

(E) Density plots depicting CD107a (*top*) and IFN-γ (*bottom*) expression in response to GBM43-WT cells by sorted TIGIT^{high}, TIGIT^{medium}, and TIGIT^{negative} NK cells at E:T ratios 2.5:1, 5:1, and 10:1.

(F) Glycolysis levels (L-lactate concentration; mM) in cell culture supernatant of TIGIT^{high}, TIGIT^{medium}, and TIGIT^{negative} NK cells cultured for 24 or 48 h (n = 2). Groups were compared using ordinary one-way ANOVA and Tukey's post-hoc test. Data are represented as mean ± SEM. *p < *0.05*, **p < *0.01*, ***p < *0.001*, ****p < *0.0001*.

Loss of CD155 affects GBM tumor growth and results in NK cell hyperactivation *in vivo*

CD155 is one of the main TIGIT ligands. Based on our data, we hypothesized that TIGIT does not possess an ability to itself send inhibitory signals but rather respond to dominating ligands it binds to, and we were interested in finding out if this was true for its interactions with CD155. To assess the effect of CD155 on TIGIT-induced modulation of NK cell function and establish the role of the TIGIT-CD155 axis in NK cell activity, we generated a GBM43 CD155-knockdown (KD) cell line (Figures S15 and S16). Loss of CD155 significantly inhibited proliferation of GBM43 cells (Figure 5A). Further, dual blockade of TIGIT and CD155 was able to enhance NK cell lysis of GBM43 cells *in vitro*, over NK cell controls (Figure 5B).

In summary, *in vitro* data suggested that loss of CD155 was detrimental to GBM growth. To assess the effect of loss of CD155 on GBM cells *in vivo*, we established a subcutaneous GBM43 xenograft model in both NRG and RAG1$^{-/-}$ mice (Figure 5C). Loss of CD155 inhibited GBM43 tumor growth in NRG mice (Figures 5D and 5E). In RAG1$^{-/-}$ mice, where innate immune cell activity contributes to anti-tumor responses, we observed that loss of CD155, coupled with immune cell activity which includes NK cells and other innate immune cells, could nearly eliminate GBM43 tumor growth altogether (Figures 5D, 5E, and S17). Following this study, we harvested cNK and tiNK, cells from RAG1$^{-/-}$ mice for phenotyping and functional assays. cNK cells from CD155-KD tumor-bearing RAG1$^{-/-}$ mice exhibited higher levels of TIGIT than PBS control mice (Figures 5F, 5G, S18, and S19). On the other hand, tiNK cells from CD155-KD mice had higher levels of DNAM-1, LAG-3, CD96, and TIGIT, and lower levels of CD16/32 (Figures 5F and 5G). These data indicate that TIGIT follows NK cell activation, does not mark NK cell dysfunction and benefits from lack of CD155. cNK cells were predominantly CD11b^{-}CD27^{-}, indicating an inactive, naive phenotype. However, tiNK cells had comparatively higher levels of CD27^{+} and CD11b^{+} NK cells, suggesting NK cell maturation. CD155-KD tumor-bearing RAG1$^{-/-}$ mice had significantly higher levels of CD27^{+} tiNK cells than WT tumor-bearing RAG1$^{-/-}$ mice, indicative of heightened cytokine secretion, but lower cytolytic function. We also assessed the number and functional activity of tiNK cells through IHC staining of NKp46 and Granzyme B and found that CD155 KD tumors had higher numbers of tiNK cells expressing NKp46 (WT: 3.25 ± 1.03 cells/frame; KD: 48.25 ± 4.27 cells/frame) and Granzyme B (WT: 6.50 ± 1.44 cells/frame; KD: 24.50 ± 5.42 cells/frame) than WT GBM tumors, suggesting that loss of CD155 could promote NK cell activity and trafficking (Figure 5H). cNK cells also exhibited no differences in cytolysis of GBM43 WT cells (Figure S20). Overall, these studies confirmed that TIGIT does not mark NK cell dysfunction in GBM and are consistent with our notion of it acting in contexts of competitive binding, liberating NK cell activity when its dominating binding partner is absent.

TIGIT blockade relies on 4-1BB activity

Having observed that TIGIT blockade induced upregulation of 4-1BB on NK cells, we explored 4-1BB for its role as a potential co-expressed receptor in regulating NK cell responses to modulation of TIGIT. Our data showed that neither blockade of TIGIT alone, nor blockade of 4-1BB alone, nor co-blockade of both receptors together could effectively enhance NK cell cytolytic activity against GBM (GBM43, U87MG, GBM10) *in vitro* (Figures 6 and S21). However, blockade of TIGIT, coupled with 4-1BB stimulation with an agonistic mAb, significantly enhanced NK cell cytolytic activity against patient-derived GBM43 targets, while either treatment alone did not generate a significant response (Figures 6B and S21). These observations suggested that 4-1BB stimulation could be relying on TIGIT blockade to enhance NK cell function against cancer targets, and that the two might be acting as related immunomodulators.

We next assessed the efficacy of dual-targeting of TIGIT and 4-1BB in a subcutaneous xenograft model, established with CD155^{+} primary patient-derived GBM43 WT cells (tumor cells used within 10 passages after primary isolation from the patient). Treatment with human NK cells and rhIL-15, in combination with both TIGIT blockade and 4-1BB stimulation, was most effective is suppressing growth of GBM43-WT tumors *in vivo* (Figures 6C–6G and S22) compared to all other treatment groups. Treatment of tumor-bearing mice with IL-15-stimulated human NK cells resulted in limited control of tumor growth. Similarly, blockade of TIGIT alone was not effective in restricting tumor growth, nor was agonism of 4-1BB alone, compared to mice receiving IL-15-stimulated human NK cells. There was also no significant decrease in mouse bodyweight over the course of the of the study (Figure 6G). Though significant, the overall effect of tumor growth upon 4-1BB agonism/TIGIT blockade was modest at best, suggesting that while important, the contribution of 4-1BB to the *in vivo* activation of anti-TIGIT responses likely involves other signaling co-receptor activities. Nonetheless, our data revealed a non-trivial contributory role of 4-1BB to TIGIT immunotherapy and potential reasoning for failure of TIGIT monotherapy. Following treatments, mouse blood and tumors were harvested and tiNK cells isolated for assessment by flow cytometry of a panel of functional receptors (CD16, CD69, DNAM-1, NKG2D, NKp30, CD96, 4-1BB, CD158b, CD158e1, TIGIT, CD57 NKG2A/CD94, LAG-3, PD-1, TIM-3). Phenotypic analysis demonstrated no major difference in cell numbers in any

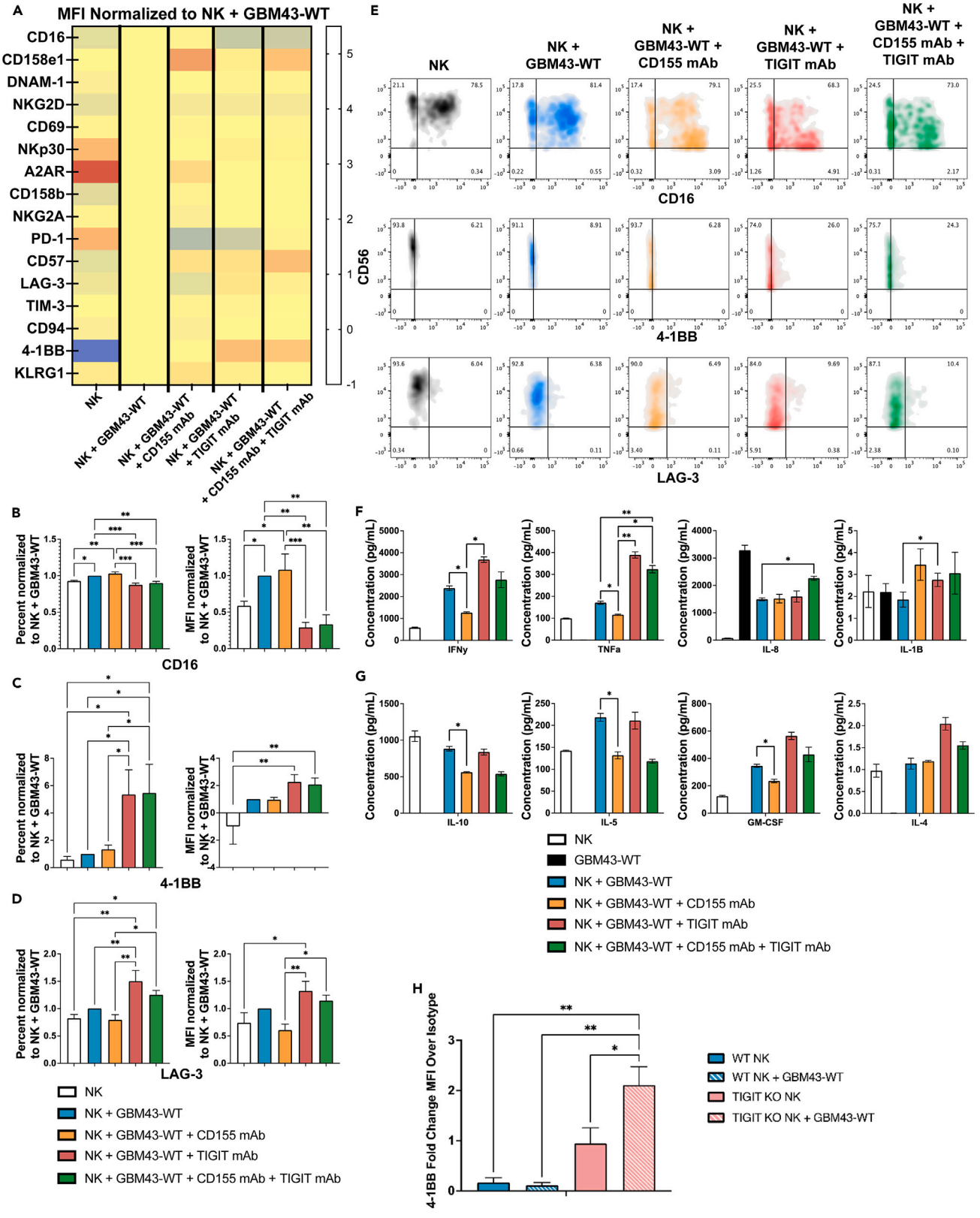
A
MFI Normalized to NK + GBM43-WT
CD16
CD158e1
DNAM-1
NKG2D
CD69
NKp30
A2AR
CD158b
NKG2A
PD-1
CD57
LAG-3
TIM-3
CD94
4-1BB
KLRG1
NK
NK + GBM43-WT
NK + GBM43-WT + CD155 mAb
NK + GBM43-WT + TIGIT mAb
NK + GBM43-WT + CD155 mAb + TIGIT mAb
E
NK
NK + GBM43-WT
NK + GBM43-WT + CD155 mAb
NK + GBM43-WT + TIGIT mAb
NK + GBM43-WT + CD155 mAb + TIGIT mAb
CD16
CD56
4-1BB
LAG-3
B
Percent normalized to NK + GBM43-WT
MFI normalized to NK + GBM43-WT
CD16
C
4-1BB
D
LAG-3
F
Concentration (pg/mL)
IFNγ
TNFa
IL-8
IL-1B
G
IL-10
IL-5
GM-CSF
IL-4
NK
GBM43-WT
NK + GBM43-WT
NK + GBM43-WT + CD155 mAb
NK + GBM43-WT + TIGIT mAb
NK + GBM43-WT + CD155 mAb + TIGIT mAb
H
4-1BB Fold Change MFI Over Isotype
WT NK
WT NK + GBM43-WT
TIGIT KO NK
TIGIT KO NK + GBM43-WT

Figure 4. TIGIT blockade correlates with low CD16, high 4-1BB, and higher inflammatory cytokines

(A) Heatmap depicting normalized MFI expression of NK cell activating (CD16, DNAM-1, NKG2D, CD69, NKp30, CD57, 4-1BB) and inhibitory (CD158e1, CD158b, NKG2A, PD-1, LAG-3, CD94, A2AR, TIM-3, KLRG1) receptors on NK cells cocultured with GBM43 cells, with or without CD155 and/or TIGIT mAb blockade (n = 3).

(B) CD16, (C) 4-1BB, (D) and LAG-3 percentage (*left*) and MFI (*right*) expression on NK cells co-cultured with GBM43-WT cells, with or without CD155 and/or TIGIT mAb blockade (n = 3). Groups were compared using ordinary one-way ANOVA and Tukey's post-hoc test.

(E) Density plots depicting CD16, 4-1BB and LAG-3 expression on NK cells co-cultured with GBM43 cells, with or without CD155 and/or TIGIT mAb blockade. Levels of proinflammatory cytokines (F) IFN-γ, TNF-α, IL-8, IL-1β (G) IL-10, IL-5, GM-CSF, and IL-4 in cell supernatant of NK cells co-cultured with GBM43-WT cells, with or without CD155 and/or TIGIT mAb blockade (n = 3). Groups were compared using ordinary one-way ANOVA and Tukey's post-hoc test.

(H) Change in expression (measured as MFI fold over isotype control) of 4-1BB on $TIGIT^{KO}$ and WT NK cells generated via CRISPR/Cas9 editing in the absence and presence of GBM43 cells (incubated as co-culture at an E:T 2.5:1). Groups were compared using ordinary one-way ANOVA and Tukey's post-hoc test. Data are represented as mean ± SEM. *p < *0.05*, **p < *0.01*, ***p < *0.001*, ****p < *0.0001*.

of the treatment groups (PBS group contained no NK cells) (Figure 6F). When comparing antibody treatment groups against NK cell therapy alone, tiNK cells from the TIGIT + 4-1BB co-therapy group (TIGIT blockade + 4-1BB agonism) showed significantly higher expression of CD158e1, DNAM-1, CD96, and NKG2A, and lower expression of TIM-3 and TIGIT (Figures 6H, 6I, S1, and S23).

DISCUSSION

TIGIT has been described as a checkpoint receptor on NK cells,[15] contributing to its emergence as an immunotherapeutic target. However, studies on its role as a checkpoint receptor have produced disparate data: on one hand, TIGIT monotherapy has been shown to be effective in controlling tumor growth in only limited mouse tumor models,[14] while, elsewhere, its effectiveness as a checkpoint target failed, instead requiring co-stimulation of NK cells with cytokines or co-blockade of additional checkpoint receptors such as PD-1[12,13] for the induction of functional responses. It is the interaction between TIGIT and cancer-associated CD155[27] that dominates the inhibitory functions induced by TIGIT on NK cells 36). However, NK cell receptors CD226 (DNAM-1) and CD96 also bind to CD155 and promote additional or competing NK cell activating and inhibitory functions. The heterogeneous responses to TIGIT blockade and the poor success of its targeting via checkpoint blockade have prompted us to investigate its role on NK cells and on the modulation of NK cell anti-tumor responses. Our findings have indicated that TIGIT is a heterogeneous receptor on NK cells that does not directly inhibit NK cells through signaling, but competitively usurps NK cell effector responses and is involved in the regulation of activating ligand expression, and not a marker of NK cell dysfunction or exhaustion in GBM.

Overall, our studies have uncovered a novel co-expression relationship between 4-1BB and TIGIT. Not only did expression of TIGIT correlate with expression of 4-1BB – and not of other NK cell receptors – in GBM patients, but successful functional targeting of TIGIT correlated with activity and enhanced expression of 4-1BB. In other words, the association between TIGIT and 4-1BB was observed mainly at the expression level in patient samples and *in vitro* assays, however co-expression was also noted in response to blockade of TIGIT/CD155, hinting at a potential co-signaling relationship. Loss of TIGIT on NK cells, conversely, abrogated these effects. Analysis of TCGA data also indicated a positive correlation between TIGIT and 4-1BB expression in GBM patient data (Spearman's correlation = 0.414, Figure S24). Further, in our patient phenotyping studies we observed a strong correlation between TIGIT and 4-1BB expression in both cNK and tiNK cells from GBM patients. The nature of the functional and mechanistic relationship between these two receptors remains to be elucidated. Likewise, our findings do not preclude involvement of other receptors that communicate with TIGIT. The "decoy-like" designation stems from the observed behavior wherein TIGIT does not appear to innately and spontaneously send inhibitory signals to NK cells upon engagement of CD155, but rather prevents binding of CD155 with DNAM-1, as well as induces downregulation of other activating receptors upon CD155 engagement. Therefore, targeting of TIGIT via antibody blockade does not prevent inhibitory signaling but rather encourages binding of the activating co-receptors for the same ligands and promotes expression of other NK activating receptors, namely 4-1BB. Therefore, effective targeting of TIGIT with NK cell therapy requires blockade of TIGIT coupled with stimulation of NK cell functional responses, through stimulation of activating ligands or with cytokines. Blocking TIGIT on human NK cells *in vitro* resulted in phenotypic changes which included a strong upregulation of 4-1BB, further hinting at a correlation between 4-1BB and TIGIT on NK cells. Such upregulation of 4-1BB was true for NK cells lacking the expression of TIGIT ($TIGIT^{KO}$ NK cells), and was further confirmed when we sorted human NK cells. This indicated that, overall, $TIGIT^{+}$ ($TIGIT^{high}$ and $TIGIT^{medium}$) NK cells had enhanced functionality compared to NK cells lacking this receptor. Interestingly, the receptor TIM-3 was also upregulated on $TIGIT^{+}$ NK cells. We had previously found that TIM-3 correlated with a higher capacity to produce IFN-γ,[28] similarly linking this receptor to an activating role on NK cells. Its involvement in IFN-γ activity on $TIGIT^{+}$ NK cells is unclear, however, our data further indicate that these cells possess a higher functional capacity which correlated with a more pronounced $TIM\text{-}3^{+}$ phenotype. Further corroborating these observations, through gene expression analysis we found that $TIGIT^{+}$ NK cells were marked by heightened *TNFRSF9* (4-1BB) expression and a transcriptional signature indicative of mature and functional cells compared to $TIGIT^{-}$ NK cells. These are not isolated observations: studies have indicated that $TIGIT^{+}$ NK cells isolated for patients were more mature and had a higher cytolytic potential compared to $TIGIT^{negative}$ NK cells,[13] and that TIGIT promotes maturation of NK cells while imparting these cells with a higher cytolytic capacity.[29]

As a co-stimulatory receptor on NK cells, 4-1BB has a recognized role in triggering NK cell proliferation.[30] The interactions between 4-1BB—4-1BBL were previously reported to protect tumor cells from NK cell-mediated killing,[31] promoting the notion of an inhibitory role of 4-1BB on NK cells in leukemia. In the context of the role of 4-1BB stimulation alone on NK cell killing, other studies have pointed out either the lack of its ability to enhance cytolytic activity of NK cells,[30] a detrimental effect on their function,[32] or, conversely, its ability to enhance ADCC upon FC-receptor ligation[33] and enhance TNF-α secretion.[34] Our observations in solid tumors suggest the former—4-1BB agonism alone had no effect on the cytolytic activity of PNK cells against GBM cells. We found that agonism of 4-1BB alongside the blockade of TIGIT was superior to either

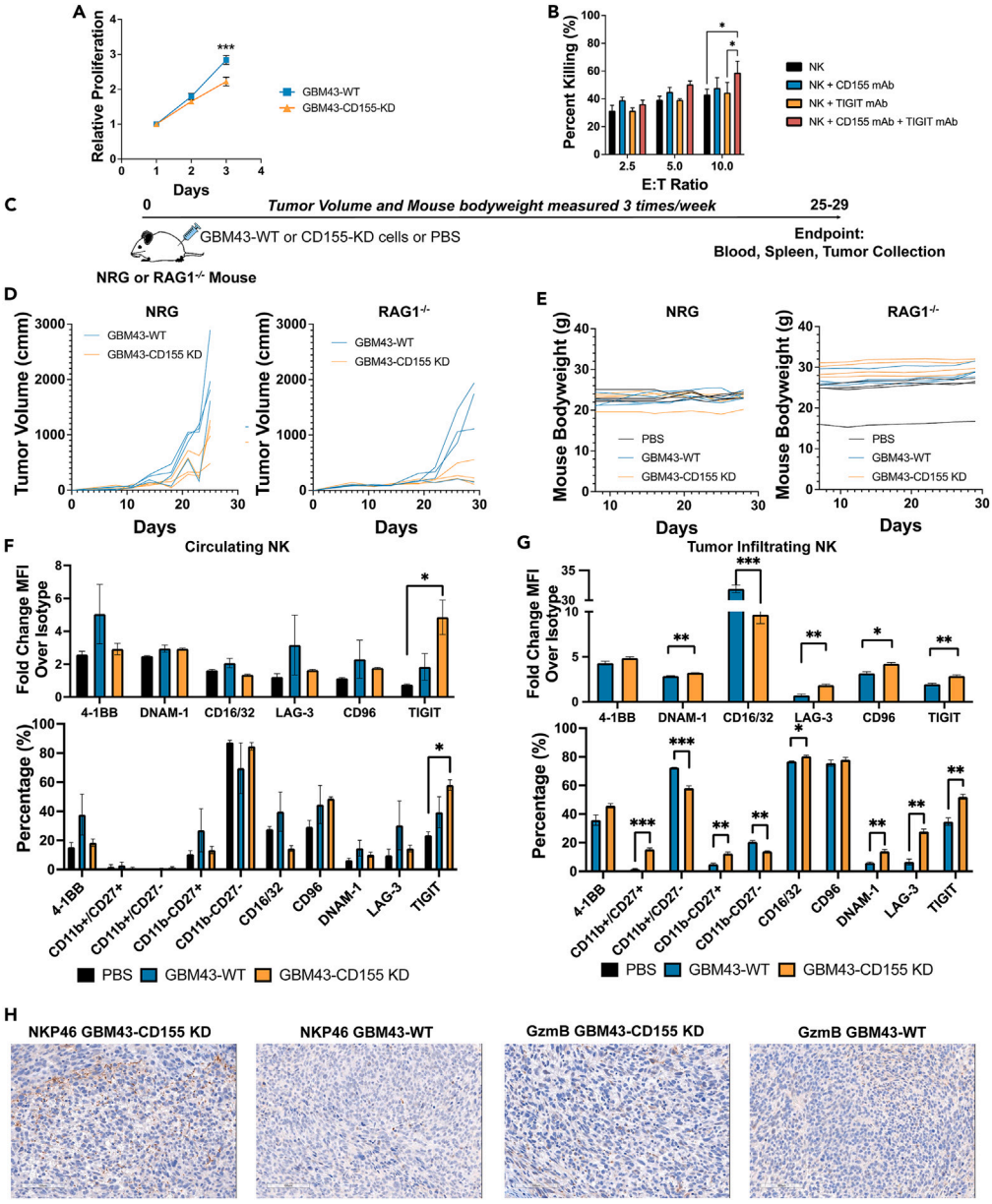

Figure 5. Loss of CD155 affects GBM tumor growth and results in NK cell hyperactivation in vivo

(A) Relative proliferation of GBM43-WT and GBM43-CD155 KD cells (n = 3) measured via CCK-8 proliferation assay. Groups were compared using an unpaired Student's *t* test at each timepoint indicated.

(B) NK cell-induced cytolysis of GBM43-WT cells, with or without CD155 and/or TIGIT mAb blockade, at E:T ratios of 2.5:1, 5:1, and 10:1 (n = 3). Groups were compared using ordinary one-way ANOVA and Tukey's post-hoc test.

(C) *In vivo* study timeline. Timeline depicting tumor inoculation, tumor growth measurement, and tumor harvesting in GBM43 NRG and RAG1$^{-/-}$ mouse xenografts.

(D) Tumor volume measurements of NRG *(left)* or RAG1$^{-/-}$ *(right)* mice bearing either GBM43-WT tumors, GBM43-CD155 KD tumors, or no tumors (n = 4).

(E) Bodyweight measurements of NRG *(left)* or RAG1$^{-/-}$ *(right)* mice bearing either GBM43-WT tumors, GBM43-CD155 KD tumors, or no tumors (n = 4).

(F) MFI *(top)* and percentage *(bottom)* expression of NK cell receptors on cNK cells harvested from RAG1$^{-/-}$ mice (n = 4). Groups were compared using ordinary one-way ANOVA and Tukey's post-hoc test.

(G) MFI *(top)* and percentage *(bottom)* expression of NK cell receptors on tiNK cells harvested from RAG1$^{-/-}$ mice (n = 4). Groups were compared using unpaired Student's *t* test for each ligand tested.

(H) IHC staining of NKp46 and Granzyme B, in GBM43-WT and GBM43-CD155 KD tumor sections harvested from RAG1$^{-/-}$ mice. Scale bar: 100 μm. Data are represented as mean ± SEM. *p < *0.05*, **p < *0.01*, ***p < *0.001*, ****p < *0.0001*.

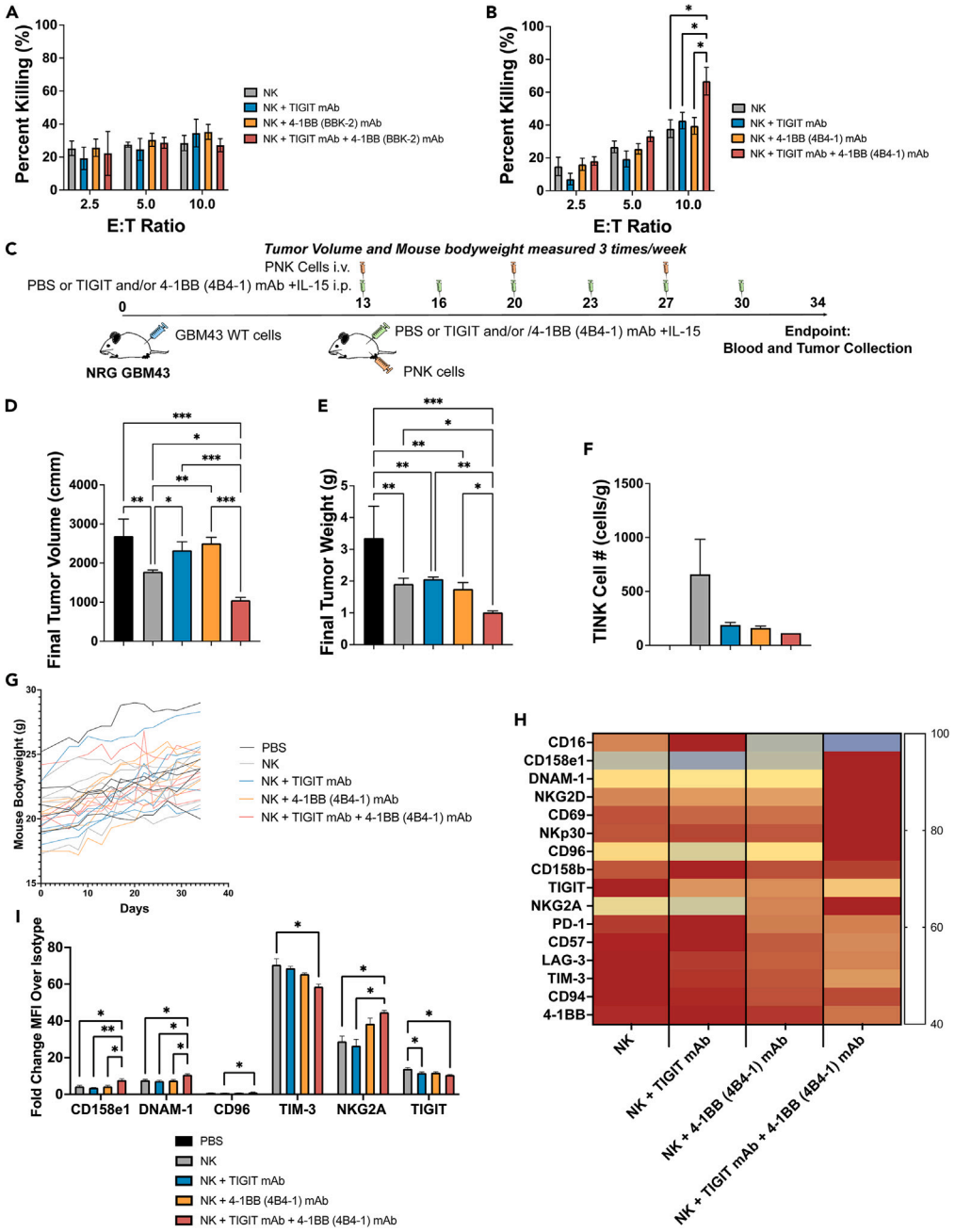

Figure 6. TIGIT blockade relies on 4-1BB activity

(A) Cytolysis of GBM43-WT cells by NK cells with or without TIGIT and/or 4-1BB (BBK-2) mAb blockade at E:T ratios 2.5:1, 5:1, and 10:1 (n = 4). Groups were compared using ordinary one-way ANOVA and Tukey's post-hoc test.

(B) Cytolysis of GBM43-WT cells by NK cells with or without TIGIT and/or 4-1BB agonistic (4B4-1) mAb treatment at E:T ratios 2.5:1, 5:1, and 10:1 (n = 4). Groups were compared using ordinary one-way ANOVA and Tukey's post-hoc test.

(C) *In vivo* study timeline. Timeline depicting tumor inoculation, NK cell adoptive transfer and mAb administration, tumor and bodyweight measurement, and tumor harvesting in GBM43 NRG mouse xenografts.

(D) Final tumor volume, (E) final tumor weight, and (F) tumor-infiltrating NK cell number of NRG mice bearing GBM43-WT tumors, receiving NK cells with or without TIGIT and/or 4-1BB agonistic (4B4-1) mAb, or PBS (n = 5). Groups were compared using ordinary one-way ANOVA and Tukey's post-hoc test.

(G) Bodyweight measurement of NRG mice bearing GBM43-WT tumors, receiving adoptively-transferred NK cells with or without TIGIT blocking and/or 4-1BB agonistic (4B4-1) mAb, or PBS (n = 5).

Figure 6. *Continued*

(H) Heatmap depicting normalized MFI expression of NK cell receptors on NK cells harvested from NRG mice bearing GBM43-WT tumors, treated with adoptively-transferred NK cells with or without TIGIT blocking and/or 4-1BB agonistic (4B4-1) mAb (n = *5 per group*).

(I) Expression levels, on NK cells harvested from treated GBM43-bearing mice, of select NK cell receptors showing differential expression between NK cell adoptive transfer + mAb treatments and control NK cell groups (n = 5). Groups were compared using ordinary one-way ANOVA and Tukey's post-hoc test. Data are represented as mean ± SEM. *p < *0.05*, **p < *0.01*, ***p < *0.001*, ****p < *0.0001*.

treatment alone in controlling growth of GBM tumors *in vivo*, likely due to the upregulation of 4-1BB induced by TIGIT blockade in the presence of GBM cells, but was not sufficient in arresting tumor growth. This suggests that the involvement of TIGIT's competitive inhibition of activating co-receptors, rather than inhibitory signaling alone. Our data also suggest that TIGIT acts to suppress overexpression of 4-1BB, and likely other receptors, when stimulated by $CD155^+$ GBM cells, and the lack of TIGIT signaling in the settings of TIGIT blockade fully liberates 4-1BB expression, enhancing NK cytolytic responses upon 4-1BB stimulation. This relationship in the context of NK cell activation also makes sense when considering the role of 4-1BB in NK cell activation. This confirms that TIGIT's inhibitory role is context-specific and is driven, in part, by interactions with inhibitory binding partners (CD155), while also inducing inhibition through interference with activating receptors, co-expressed alongside TIGIT. Though a combination of IL-15 and TIGIT blockade resulted in anti-tumor activity in recent studies,[17] we observed limited responses to this treatment combination. Different treatment schedules or dosages might be needed to elicit anti-tumor activity against GBM, or different ligand-receptor dynamics could be in play in this tumor.

Our study also highlighted the potent role of the non-MHC class I ligand CD155 in modulating TIGIT-dependent NK cell responses and its involvement in TIGIT's inhibitory roles. CD155 does not, however, perform this role in isolation, and its effects on GBM are distinct from those it has on NK cells, where it competes with other functional ligands. Not only do our data indicate that loss of CD155 impairs GBM tumor growth, but it could be inducing upregulation of its binding partners on NK cells, as a compensatory mechanism for its loss. In line with this, we hypothesize that CD155 might be the dominant driver of TIGIT-induced NK cell inhibition in solid tumors via signaling along TIGIT's immunoreceptor tyrosine-based inhibitory motif in its cytoplasmic portion. However, we saw no effect to NK cell anti-tumor activity upon blockade of CD155 *in vitro*. It is possible that, in isolation, CD155-dependent inhibition of NK cells is insufficient in overcoming NK cell activating signals, yet benefits from additional inhibitory signals, and possible NK cell dysfunction, that occurs in the tumor microenvironment. We and others have shown that loss of NK cell activity, most obviously through the downregulation of activating receptors, is a common feature of tiNK cells. Interestingly, loss of CD155 on tumor cells rendered NK cells hypofunctional against cancer targets, suggesting that TIGIT-CD155 engagement might be required for triggering NK cell-mediated cytolysis, a notion that has been suggested in other studies.[29] Altogether this highlights the complex network of cancer ligands (CD155, CD112, etc.) and NK cell receptors (TIGIT, DNAM-1,CD96, 4-1BB) involved in signaling within the CD155-TIGIT axis, and why immunotherapies targeting TIGIT or CD155 alone, have had limited clinical efficacy.

That blocking TIGIT in the presence of cancer cells—where it is free to bind to inhibitory receptor CD155—required agonism of 4-1BB, but not its blockade, might be indicative of the fact that 4-1BB functions as an activating receptor on NK cells in GBM, and that it actively responds to blockade of TIGIT. More so, it points to a relationship that exists between 4-1BB and TIGIT on NK cells, as we have shown, both phenotypically and transcriptionally. However, the involvement of 4-1BB-independent mechanisms in regulating responses to TIGIT is also likely. It is important to note that many of our analyses utilized sorted $TIGIT^+$ NK cells, which represent a subset of NK cells found in peripheral blood. As such, global responses would not be reflective only of these cells' activity. We also note, based on our *in vivo* data, that TIGIT signaling in the tumor setting activates complex receptor-ligand interactions which dominate over those induced by $TIGIT^+$ NK cells alone.

More broadly, our studies suggest that TIGIT regulates a complex binding network on NK cells in GBM, and acts competitively with other ligands, regulates expression of some of them, but does not by itself spontaneously induce inhibitory signaling, giving reason to the poor responses observed to TIGIT blockade alone. Specifically, TIGIT acts as a complex heterogeneous receptor on NK cells with signaling partners that go beyond CD155, CD112 and CD226 and include, as we have found, 4-1BB. The balance of the signaling between its ligands ultimately directs its effect on NK cell function. The functional capacity of $TIGIT^+$ NK cells to drive NK cell function and higher cytolytic capacity might promote their use as cytolytic effectors in a therapeutic setting. At the same time, immunotherapeutic targeting of TIGIT, while cancer-specific, requires blockade of TIGIT itself, coupled with modulation of one of its, potentially many, signaling partners, including 4-1BB, to elicit full responses. Our study, however, does not define 4-1BB as the sole regulator of TIGIT responses, but nonetheless reveals an important contributory role for 4-1BB in TIGIT immunotherapy, while providing important direct clues as to the ineffectiveness of anti-TIGIT monotherapy.

Limitations of the study

Though we have shown, using GBM patient data, *in vivo* human patient-derived GBM xenografts and multiple pharmacological and genetic knockout models to study the role and loss of TIGIT and its ligand CD155 alongside agonism of 4-1BB, that TIGIT is a heterogeneous receptor, rather than a driver of NK cell dysfunction, this study has a number of limitations which could be addressed in follow-up work. First, additional follow-up *in vivo* studies in immunocompetent orthotopic models could not only validate, but also shed more comprehensive insight into the role of the GBM microenvironment on NK cell function in the context of TIGIT signaling and activation. In addition, employing transgenic mouse models would enable the targeted study of the molecular and immunological mechanisms underpinning the role of TIGIT on NK

cells described in this study. Further efficacy studies employing agonism of 4-1BB in combination with TIGIT and/or CD155 blockade in orthotopic humanized mouse models would validate the findings reported here in physiologically relevant settings.

STAR★METHODS

Detailed methods are provided in the online version of this paper and include the following:

- KEY RESOURCES TABLE
- RESOURCE AVAILABILITY
  - Lead contact
  - Materials availability'
  - Data and code availability
- EXPERIMENTAL MODEL AND STUDY PARTICIPANTS DETAILS
- METHOD DETAILS
  - Human NK cell isolation from peripheral blood and culture
  - Cell lines and culture
  - GBM patient samples
  - Cell sorting and phenotyping
  - TCGA survival analysis
  - RNAseq analysis
  - Pathway analysis of RNAseq gene expression data
  - TIGIT-sorted NK cell phenotyping and function
  - Generation of CRISPR/Cas9 TIGIT knockout NK cells
  - NK cell phenotyping and cytokine screening on GBM co-culture
  - Enzyme-linked immunosorbent assay
  - CD155 knockdown in GBM
  - CD155 pharmacological inhibition assays
  - *In vivo* GBM CD155 KD studies and NK cell analysis
  - Histological analysis
  - 4-1BB cytolysis assays
  - *In vivo* 4-1BB/TIGIT targeting in GBM and tumor-infiltrating NK cell analysis
- QUANTIFICATION AND STATISTICAL ANALYSIS

SUPPLEMENTAL INFORMATION

Supplemental information can be found online at https://doi.org/10.1016/j.isci.2023.108353.

ACKNOWLEDGMENTS

This work was supported by National Institutes of Health grant 1 R21CA256413-01 from the National Cancer Institute, the V Foundation for Cancer Research (Grant #D2019-039), the Walther Cancer Foundation (Embedding Tier I/II Grant #0186.01) and a McKeehan Graduate Fellowship to Kyle Lupo. The authors also gratefully acknowledge the support of the Collaborative Core for Cancer Bioinformatics, the Biological Evaluation Shared Resource and the Flow Cytometry Shared Resource, with support from the Purdue Center for Cancer Research, NIH grant P30 CA023168, the IU Simon Cancer Center NIH grant P30 CA082709, and the Walther Cancer Foundation.

AUTHOR CONTRIBUTIONS

K.B.L. and S.M. conceived, designed, and executed the experiments and wrote the manuscript; B.E. and S.T-A. maintained mice and carried out *in vivo* xenograft studies; N.A.L. and S.U. performed bioinformatics analysis; M.M. performed histological analysis; K.P. helped establish *in vivo* mouse models; K.P. helped establish patient-derived GBM lines; A.C.G. and V.S. collected and prepared patient GBM samples. all authors reviewed and edited the manuscript.

DECLARATION OF INTERESTS

The authors declare no competing interests.

Received: May 22, 2023
Revised: August 27, 2023
Accepted: October 24, 2023
Published: October 28, 2023

REFERENCES

1. Lupo, K.B., and Matosevic, S. (2019). Natural Killer Cells as Allogeneic Effectors in Adoptive Cancer Immunotherapy. Cancers *11*, 769. https://doi.org/10.3390/cancers11060769.
2. Merino, A., Zhang, B., Dougherty, P., Luo, X., Wang, J., Blazar, B.R., Miller, J.S., and Cichocki, F. (2019). Chronic stimulation drives human NK cell dysfunction and epigenetic reprograming. J. Clin. Invest. *129*, 3770–3785. https://doi.org/10.1172/JCI125916.
3. Ndhlovu, L.C., Lopez-Vergès, S., Barbour, J.D., Jones, R.B., Jha, A.R., Long, B.R., Schoeffler, E.C., Fujita, T., Nixon, D.F., and Lanier, L.L. (2012). Tim-3 marks human natural killer cell maturation and suppresses cell-mediated cytotoxicity. Blood *119*, 3734–3743. https://doi.org/10.1182/blood-2011-11-392951.
4. Dao, T.N., and Matosevic, S. (2019). Immunometabolic Responses of Natural Killer Cells to Inhibitory Tumor Microenvironment Checkpoints. Immunometabolism *1*, e190003. https://doi.org/10.20900/immunometab20190003.
5. Stanietsky, N., Simic, H., Arapovic, J., Toporik, A., Levy, O., Novik, A., Levine, Z., Beiman, M., Dassa, L., Achdout, H., et al. (2009). The interaction of TIGIT with PVR and PVRL2 inhibits human NK cell cytotoxicity. Proc. Natl. Acad. Sci. USA *106*, 17858–17863. https://doi.org/10.1073/pnas.0903474106.
6. Manieri, N.A., Chiang, E.Y., and Grogan, J.L. (2017). TIGIT: A Key Inhibitor of the Cancer Immunity Cycle. Trends Immunol. *38*, 20–28. https://doi.org/10.1016/j.it.2016.10.002.
7. Liu, S., Zhang, H., Li, M., Hu, D., Li, C., Ge, B., Jin, B., and Fan, Z. (2013). Recruitment of Grb2 and SHIP1 by the ITT-like motif of TIGIT suppresses granule polarization and cytotoxicity of NK cells. Cell Death Differ. *20*, 456–464. https://doi.org/10.1038/cdd.2012.141.
8. Sarhan, D., Cichocki, F., Zhang, B., Yingst, A., Spellman, S.R., Cooley, S., Verneris, M.R., Blazar, B.R., and Miller, J.S. (2016). Adaptive NK Cells with Low TIGIT Expression Are Inherently Resistant to Myeloid-Derived Suppressor Cells. Cancer Res. *76*, 5696–5706. https://doi.org/10.1158/0008-5472.CAN-16-0839.
9. Stanietsky, N., Rovis, T.L., Glasner, A., Seidel, E., Tsukerman, P., Yamin, R., Enk, J., Jonjic, S., and Mandelboim, O. (2013). Mouse TIGIT inhibits NK-cell cytotoxicity upon interaction with PVR. Eur. J. Immunol. *43*, 2138–2150. https://doi.org/10.1002/eji.201243072.
10. He, Y., and Tian, Z. (2017). NK cell education via nonclassical MHC and non-MHC ligands. Cell. Mol. Immunol. *14*, 321–330. https://doi.org/10.1038/cmi.2016.26.
11. Johnston, R.J., Comps-Agrar, L., Hackney, J., Yu, X., Huseni, M., Yang, Y., Park, S., Javinal, V., Chiu, H., Irving, B., et al. (2014). The Immunoreceptor TIGIT Regulates Antitumor and Antiviral CD8+ T Cell Effector Function. Cancer Cell *26*, 923–937. https://doi.org/10.1016/j.ccell.2014.10.018.
12. Chauvin, J.-M., Pagliano, O., Fourcade, J., Sun, Z., Wang, H., Sander, C., Kirkwood, J.M., Chen, T.h.T., Maurer, M., Korman, A.J., and Zarour, H.M. (2015). TIGIT and PD-1 impair tumor antigen-specific $CD8^+$ T cells in melanoma patients. J. Clin. Invest. *125*, 2046–2058. https://doi.org/10.1172/JCI80445.
13. Chauvin, J.-M., Ka, M., Pagliano, O., Menna, C., Ding, Q., DeBlasio, R., Sanders, C., Hou, J., Li, X.-Y., Ferrone, S., et al. (2020). IL15 Stimulation with TIGIT Blockade Reverses CD155-mediated NK-Cell Dysfunction in Melanoma. Clin. Cancer Res. *26*, 5520–5533. https://doi.org/10.1158/1078-0432.CCR-20-0575.
14. Zhang, Q., Bi, J., Zheng, X., Chen, Y., Wang, H., Wu, W., Wang, Z., Wu, Q., Peng, H., Wei, H., et al. (2018). Blockade of the checkpoint receptor TIGIT prevents NK cell exhaustion and elicits potent anti-tumor immunity. Nat. Immunol. *19*, 723–732. https://doi.org/10.1038/s41590-018-0132-0.
15. Maas, R.J., Hoogstad-van Evert, J.S., Van der Meer, J.M., Mekers, V., Rezaeifard, S., Korman, A.J., de Jonge, P.K., Cany, J., Woestenenk, R., Schaap, N.P., et al. (2020). TIGIT blockade enhances functionality of peritoneal NK cells with altered expression of DNAM-1/TIGIT/CD96 checkpoint molecules in ovarian cancer. OncoImmunology *9*, 1843247. https://doi.org/10.1080/2162402X.2020.1843247.
16. Xu, F., Sunderland, A., Zhou, Y., Schulick, R.D., Edil, B.H., and Zhu, Y. (2017). Blockade of CD112R and TIGIT signaling sensitizes human natural killer cell functions. Cancer Immunol. Immunother. *66*, 1367–1375. https://doi.org/10.1007/s00262-017-2031-x.
17. Judge, S.J., Darrow, M.A., Thorpe, S.W., Gingrich, A.A., O'Donnell, E.F., Bellini, A.R., Sturgill, I.R., Vick, L.V., Dunai, C., Stoffel, K.M., et al. (2020). Analysis of tumor-infiltrating NK and T cells highlights IL-15 stimulation and TIGIT blockade as a combination immunotherapy strategy for soft tissue sarcomas. J. Immunother. Cancer *8*, e001355. https://doi.org/10.1136/jitc-2020-001355.
18. Liu, G., Zhang, Q., Yang, J., Li, X., Xian, L., Li, W., Lin, T., Cheng, J., Lin, Q., Xu, X., et al. (2022). Increased TIGIT expressing NK cells with dysfunctional phenotype in AML patients correlated with poor prognosis. Cancer Immunol. Immunother. *71*, 277–287. https://doi.org/10.1007/s00262-021-02978-5.
19. Wang, F., Hou, H., Wu, S., Tang, Q., Liu, W., Huang, M., Yin, B., Huang, J., Mao, L., Lu, Y., and Sun, Z. (2015). TIGIT expression levels on human NK cells correlate with functional heterogeneity among healthy individuals. Eur. J. Immunol. *45*, 2886–2897. https://doi.org/10.1002/eji.201545480.
20. Jia, B., Zhao, C., Claxton, D.F., Ehmann, W.C., Rybka, W.B., Mineishi, S., Naik, S., Songdej, N., Khawaja, M., Hohl, R.J., and Zheng, H. (2018). TIGIT Expression Positively Associates with NK Cell Function in AML Patients. Blood *132*, 5250. https://doi.org/10.1182/blood-2018-99-113578.
21. Hattori, N., Kawaguchi, Y., Sasaki, Y., Shimada, S., Murai, S., Abe, M., Baba, Y., Watanuki, M., Fujiwara, S., Arai, N., et al. (2019). Monitoring TIGIT/DNAM-1 and PVR/PVRL2 Immune Checkpoint Expression Levels in Allogeneic Stem Cell Transplantation for Acute Myeloid Leukemia. Biol. Blood Marrow Transplant. *25*, 861–867. https://doi.org/10.1016/j.bbmt.2019.01.013.
22. Zhang, H., Liu, Q., Lei, Y., Zhou, J., Jiang, W., Cui, Y., He, Q., Zhu, J., Zhu, Z., Sun, Y., and Ke, Z. (2021). Direct interaction between CD155 and CD96 promotes immunosuppression in lung adenocarcinoma. Cell. Mol. Immunol. *18*, 1575–1577. https://doi.org/10.1038/s41423-020-00538-y.
23. Roman Aguilera, A., Lutzky, V.P., Mittal, D., Li, X.-Y., Stannard, K., Takeda, K., Bernhardt, G., Teng, M.W.L., Dougall, W.C., and Smyth, M.J. (2018). CD96 targeted antibodies need not block CD96-CD155 interactions to promote NK cell anti-metastatic activity. OncoImmunology *7*, e1424677. https://doi.org/10.1080/2162402X.2018.1424677.
24. Etxeberria, I., Glez-Vaz, J., Teijeira, Á., and Melero, I. (2020). New emerging targets in cancer immunotherapy: CD137/4-1BB costimulatory axis. ESMO Open *4*, e000733. https://doi.org/10.1136/esmoopen-2020-000733.
25. Reithofer, M., Rosskopf, S., Leitner, J., Battin, C., Bohle, B., Steinberger, P., and Jahn-Schmid, B. (2021). 4-1BB costimulation promotes bystander activation of human CD8 T cells. Eur. J. Immunol. *51*, 721–733. https://doi.org/10.1002/eji.202048762.
26. Zeng, T., Cao, Y., Jin, T., Tian, Y., Dai, C., and Xu, F. (2021). The CD112R/CD112 axis: a breakthrough in cancer immunotherapy. J. Exp. Clin. Cancer Res. *40*, 285. https://doi.org/10.1186/s13046-021-02053-y.
27. Anderson, A.C., Joller, N., and Kuchroo, V.K. (2016). Lag-3, Tim-3, and TIGIT: Co-inhibitory Receptors with Specialized Functions in Immune Regulation. Immunity *44*, 989–1004. https://doi.org/10.1016/j.immuni.2016.05.001.
28. Dao, T.N., Utturkar, S., Atallah Lanman, N., and Matosevic, S. (2020). TIM-3 Expression Is Downregulated on Human NK Cells in Response to Cancer Targets in Synergy with Activation. Cancers *12*, 2417. https://doi.org/10.3390/cancers12092417.
29. He, Y., Peng, H., Sun, R., Wei, H., Ljunggren, H.-G., Yokoyama, W.M., and Tian, Z. (2017). Contribution of inhibitory receptor TIGIT to NK cell education. J. Autoimmun. *81*, 1–12. https://doi.org/10.1016/j.jaut.2017.04.001.
30. Vidard, L., Dureuil, C., Baudhuin, J., Vescovi, L., Durand, L., Sierra, V., and Parmantier, E. (2019). CD137 (4-1BB) Engagement Fine-Tunes Synergistic IL-15– and IL-21–Driven NK Cell Proliferation. J. Immunol. *203*, 676–685. https://doi.org/10.4049/jimmunol.1801137.
31. Navabi, S.s., Doroudchi, M., Tashnizi, A.H., and Habibagahi, M. (2015). Natural Killer Cell Functional Activity After 4-1BB Costimulation. Inflammation *38*, 1181–1190. https://doi.org/10.1007/s10753-014-0082-0.
32. Lee, S.-H., and Hahm, D. (2016). The effects of agonistic α-4-1BB antibody on natural killer cell function. J. Immunol. *196*, 61.4.
33. Chester, C., Sanmamed, M.F., Wang, J., and Melero, I. (2018). Immunotherapy targeting 4-1BB: mechanistic rationale, clinical results, and future strategies. Blood *131*, 49–57. https://doi.org/10.1182/blood-2017-06-741041.
34. Cheuk, A.T.C., Mufti, G.J., and Guinn, B.a. (2004). Role of 4-1BB:4-1BB ligand in cancer immunotherapy. Cancer Gene Ther. *11*, 215–226. https://doi.org/10.1038/sj.cgt.7700670.
35. Wu, T., Hu, E., Xu, S., Chen, M., Guo, P., Dai, Z., Feng, T., Zhou, L., Tang, W., Zhan, L., et al. (2021). clusterProfiler 4.0: A universal enrichment tool for interpreting omics data. Innovation *2*, 100141. https://doi.org/10.1016/j.xinn.2021.100141.
36. Chen, S., Zhou, Y., Chen, Y., and Gu, J. (2018). fastp: an ultra-fast all-in-one FASTQ preprocessor. Bioinformatics *34*, i884–i890. https://doi.org/10.1093/bioinformatics/bty560.
37. Dobin, A., Davis, C.A., Schlesinger, F., Drenkow, J., Zaleski, C., Jha, S., Batut, P., Chaisson, M., and Gingeras, T.R. (2013). STAR: ultrafast universal RNA-seq aligner. Bioinformatics *29*, 15–21. https://doi.org/10.1093/bioinformatics/bts635.

38. Liao, Y., Smyth, G.K., and Shi, W. (2014). featureCounts: an efficient general purpose program for assigning sequence reads to genomic features. Bioinformatics *30*, 923–930. https://doi.org/10.1093/bioinformatics/btt656.

39. Robinson, M.D., McCarthy, D.J., and Smyth, G.K. (2010). edgeR: a Bioconductor package for differential expression analysis of digital gene expression data. Bioinformatics *26*, 139–140. https://doi.org/10.1093/bioinformatics/btp616.

40. Subramanian, A., Tamayo, P., Mootha, V.K., Mukherjee, S., Ebert, B.L., Gillette, M.A., Paulovich, A., Pomeroy, S.L., Golub, T.R., Lander, E.S., and Mesirov, J.P. (2005). Gene set enrichment analysis: A knowledge-based approach for interpreting genome-wide expression profiles. Proc. Natl. Acad. Sci. USA *102*, 15545–15550. https://doi.org/10.1073/pnas.0506580102.

41. Mootha, V.K., Lindgren, C.M., Eriksson, K.-F., Subramanian, A., Sihag, S., Lehar, J., Puigserver, P., Carlsson, E., Ridderstråle, M., Laurila, E., et al. (2003). PGC-1alpha-responsive genes involved in oxidative phosphorylation are coordinately downregulated in human diabetes. Nat. Genet. *34*, 267–273. https://doi.org/10.1038/ng1180.

STAR★METHODS

KEY RESOURCES TABLE

REAGENT or RESOURCE	SOURCE	IDENTIFIER
Antibodies		
CD3-PeCy7	BD	Clone: UCHT1; RRID:AB_2738196
CD56-PECy5.5	Thermo Fisher Scientific	Clone: CMSSB; RRID:AB_11217683
TIGIT-APC	Biolegend	Clone: A15153G; RRID:AB_2632731
DNAM-1-BV510	Biolegend	Clone: 11A8; RRID:AB_2728299
CD16-BUV395	BD	Clone 3G8; RRID:AB_2744293
NKG2A-FITC	Miltenyi Biotec	Clone: REA110; RRID:AB_2733623
CD158e1-BV421	BD	Clone: DX9; RRID:AB_2741183
PD-1-BV510	Biolegend	Clone: NAT105; RRID:AB_2721534
NKG2D-BV605	Biolegend	Clone: 1D11; RRID:AB_2728274
CD57-BV605	Biolegend	Clone: QA17A04; RRID:AB_2728425
CD69-BV650	Biolegend	Clone: FN50; RRID:AB_2563158
LAG-3-BV650	Biolegend	Clone: 11C3C65; RRID:AB_2632951
NKp30-BV711	Biolegend	Clone: P30-15; RRID:AB_2728275
TIM-3-BV711	Biolegend	Clone: F38-2E2; RRID:AB_2564045
A2AR-PE	R&D Systems	Clone: 599717
CD94-PE	Biolegend	Clone: DX22; RRID:AB_314536
CD158b-APC/Fire750	Biolegend	Clone: DX27; RRID:AB_2819943
41BB-APC/Fire750	Biolegend	Clone: 4B4-1; RRID:AB_2734280
KLRG1-APC	Biolegend	Clone: SA231A2; RRID:AB_2572161
CD96-PE	Biolegend	Clone: NK92.39; RRID:AB_2275880
NKp46-BV785	Biolegend	Clone: 9E2; RRID:AB_2810508
CD56-APC	Biolegend	Clone: CHCD56; RRID:AB_604106
TIGIT-BV421	Biolegend	Clone: A15153G; RRID:AB_2632924
IFN-γ-PerCP-Cy5.5	Biolegend	Clone: 4S.B3; RRID:AB_961355
CD107a-PE	Biolegend	Clone: H4A3; RRID:AB_1186040
m4-1BB-APC	Thermo Fisher Scientific	Clone: 17B5; RRID:AB_2573162
mCD16/32-BV421	Biolegend	Clone: 93; RRID:AB_2650889
mNK1.1-BV510	Biolegend	Clone: PK136; RRID:AB_2562217
mCD11b-BV605	Biolegend	Clone: M1/70; RRID:AB_11126744
mCD27-BV650	Biolegend	Clone: LG.3A10; RRID:AB_2687192
mCD3-BV711	Biolegend	Clone: 145-2C11; RRID:AB_2565841
mLAG-3-BV785	Thermo Fisher Scientific	Clone: C9B7W; RRID:AB_494126
mTIGIT-PE-Cy7	Biolegend	Clone: 1G9; RRID:AB_2565649
mDNAM-1-APC-Fire 750	Biolegend	Clone: 10E5; RRID:AB_2632821
4-1BB	Thermo Fisher Scientific	Clone: BBK-2; RRID:AB_10981098
TIGIT	Biolegend	Clone: A15153A; RRID:AB_2820102
CD155	Thermo Fisher Scientific	Clone: D171; RRID:AB_10978147
CD155-PE	Biolegend	Clone: SKII.4; RRID:AB_2174019
Mouse IgG1-PE	BD	Clone: MOPC-21; RRID:AB_396091
Mouse NK1.1 Monoclonal antibody	BioXCell	Clone: K136; RRID:AB_1107737
Anti-rabbit NKp46/NCR1 monoclonal antibody	R&D Systems	Cat#AF2225; RRID:AB_355192

(*Continued on next page*)

Continued

REAGENT or RESOURCE	SOURCE	IDENTIFIER
Anti-rabbit Granzyme B antibody	Abcam	Cat#Ab4059; RRID:AB_304251
Biological samples		
Human GBM patient tissue	This study	N/A
Human GBM patient blood	This study	N/A
Human donor PBMC	This study	N/A
Chemicals, peptides, and recombinant proteins		
DMEM	Gibco (Thermofisher)	Cat#11965092
Penicillin/streptomycin	Gibco	Cat#15140122
HEPES	Gibco	Cat#15630106
IL-15	Gold Biotechnology	Cat#1110-15
Sytox Green	Thermo Fisher	Cat#S7020
Sytox Blue	Thermo Fisher	Cat#S34857
DNAse I	Worthington Biochemical	Cat#LS002006
Collagenase IV	Worthington Biochemical	Cat#LS004210
Lymphoprep	STEMCELL Technologies	Cat#07801
Brefeldin A	Cayman Chemical	Cat#11861; CAS No. 20350-15-6
Monensin	Cayman Chemical	Cat#16488; CAS No. 22373-78-0
True Cut HiFI Cas9 v2	Thermo Fisher	Cat# A36498
OptiMEM	Thermo Fisher	Cat#31985062
Puromycin dihydrochloride	Alfa Aesar	Cat#4089
RPMI	Gibco	Cat#21875034
rh4-1BBL	Peprotech	Cat#310-11
RhIL-2	Akron Biotechnology	Cat#
Mitomycin C	Cayman Chemical	Cat#11435
PBS	Thermo Fisher	Cat#70011044
ACK Lysing Buffer	Thermo Fisher	Cat# A1049201
Critical commercial assays		
CytoScan LDH Assay Kit	G Bioscience	Cat#786-210
Glycolysis Cell-Based Assay kit	Cayman Chemical	Cat#600450
Human TIGIT Gene Knockout Kit v2	Synthego	GRCh38.p10
Human CD16a ELISA	Thermo Fisher	Cat#EH181RB
Mouse Cytokine Array Focused 10-plex	Eve Technologies	MDF10
Deposited data		
TCGA GBM Patient Data	TCGA	https://portal.gdc.cancer.gov/projects/TCGA-GBM
Experimental models: Cell lines		
K562	ATCC	ATCC CLL-243
U87MG	ATCC	ATCC HTB-14
GBM43	Indiana University School of Medicine	N/A
GBM10	Indiana University School of Medicine	N/A
Experimental models: Organisms/strains		
CD155 shRNA lentiviral particles	Santa Cruz	Cat#sc-61903-V
Oligonucleotides		
gRNA sequence 1: UCUUCCCUAGGAAUGAUGAC	Synthego	N/A

(*Continued on next page*)

Continued

REAGENT or RESOURCE	SOURCE	IDENTIFIER
gRNA sequence 2: AUGUCACCUCUCCUCCACCA	Synthego	N/A
gRNA sequence 3: GGCCAUUUGUAAUGCUGACU	Synthego	N/A
Software and algorithms		
R TCGAbiolinks package	Colaprico et al.	https://doi.org/10.18129/B9.bioc.TCGAbiolinks
R clusterProfiler package	Wu et al.[35]	https://doi.org/10.18129/B9.bioc.clusterProfiler
Other		
Correlative gene expression data for *TIGIT* and *TNFRSF9* (4-1BB)	cBioPortal	RNAseq V2 RSEM GBM PanCancer dataset (592 samples)
Survival analysis for GBM	GEPIA2	http://gepia2.cancer-pku.cn
Deposited data		
RNAseq NK cell TIGIThigh/low/neg gene expression data	GEO	GSE245488

RESOURCE AVAILABILITY

Lead contact

Further information and requests for reagents and resources should be directed to and will be fulfilled by the lead contact, Sandro Matosevic (sandro@purdue.edu).

Materials availability'

This study did not generate new unique reagents.

Data and code availability

- RNAseq data generated as part of this study are deposited at GEO, accession number GSE245488. TCGA GBM patient data were obtained from https://portal.gdc.cancer.gov/projects/TCGA-GBM.
- This paper does not report original code.
- Any additional information required to reanalyze the data reported in this paper is available from the lead contact upon request.

EXPERIMENTAL MODEL AND STUDY PARTICIPANTS DETAILS

Primary human NK (PNK) cells were obtained from healthy adult donors approved under Purdue University's Institutional Review Board (IRB) (IRB-approved protocol #1804020540). Ancestry, race and ethnicity were not considered when collecting samples and were not a factor in sample isolation due to requirement for donor anonymity.

GBM patient tumor and peripheral blood samples were collected by IU Health ECRO Biorepository at IU Health Methodist Hospital under Indiana University IRB protocol #1011004282 approved by the Human Subjects Office. Informed consent was obtained from all participating patients prior to undergoing surgery and procedures. For the purpose of this study, patient and donor samples were deidentified and no information on patient age or sex was obtained. In order to keep the donors confidential, no association of sex and/or gender was performed.

Male or female 6- to 12-week-old RAG1−/− mice and NOD.Cg-Prkdcscid IL2rgtm1Wjl/SzJ (NRG) mice were maintained at the Purdue Center for Cancer Research. All the animal experiments described in this study were approved by the Purdue University Animal Care and Use Committee.

METHOD DETAILS

Human NK cell isolation from peripheral blood and culture

Whole blood was collected in heparinized tubes (BD Vacutainer, 367874, BD, Franklin Lakes, NJ), untested for pathogens, and PNK cells were harvested from whole blood of adult healthy donors by negative selection, using the EasySep Direct Human NK cell Isolation Kit (StemCell Technologies, Vancouver, Canada). PNK cells were expanded for two to four weeks through coculture with K562 feeder cells (ATCC CLL-243,

Manassas, VA), treated for 3 h prior to co-culture with mitomycin C (New England Biolabs, 51854S, Ipswich, MA) to inhibit proliferation, at a 2:1 K562:NK cell ratio in RPMI media (Gibco, 21875034, Billings, MT) supplemented with 10% FBS (Corning, 35-011-CV, Corning, NY), 1% penicillin/streptomycin (Gibco, 15140122, Billings, MT), 50 ng/mL rh4-1BBL (Peprotech, 310-11, Cranbury, NJ), 50 ng/mL rhIL-21 (Gold Biotechnology, 1110-21, St. Louis, MO), and 500 IU/mL rhIL-2 (Akron Biotech, Boca Raton, FL). Prior to addition to PNK cells K562 cells were treated with 50 μg/mL of mitomycin C (Cayman Chemical, 11435, Ann Arbor, MI) for 3 h and wash with 1x PBS (Thermo Fisher Scientific, 70011044, Waltham, MA).

Cell lines and culture

Primary patient-derived GBM cells (GBM43) and recurrent patient-derived GBM cells (GBM10) cells were obtained from Dr. Karen Pollok at Indiana University School of Medicine. GBM43 and GBM10 cell lines were cultured in DMEM (Gibco, ThermoFisher, 11965092, Billings, MT) with 10% FBS and 1% HEPES (Gibco, 15630106) and maintained until passage 10 before being discarded. Chronic myelogenous leukemia K562 cells were obtained from ATCC (ATCC CLL-243, Manassas, VA). Malignant glioma U87MG cells were obtained from ATCC (ATCC HTB-14, Manassas, VA). K562 and U87MG cells were cultured in IMDM (Gibco, ThermoFisher, 12440053, Billings, MT) with 10% FBS and 1% penicillin/streptomycin (Gibco, 15140122, Billings, MT) and maintained until passage 20 before being discarded. Human rhIL-15 (1110-15) was from Gold Biotechnology.

GBM patient samples

Fresh tumor resections were stored in tissue storage buffer (Miltenyi Biotec, Gaithersrburg, MD) and processed within 24 h. Peripheral blood samples from GBM patients as well as healthy donors were collected into blood collection tubes containing sodium heparin (Vacutainer, BD, Franklin Lakes, NJ). Blood samples were processed immediately upon collection. Peripheral blood mononuclear cells (PBMCs) were isolated from peripheral whole by a Lymphoprep density gradient (StemCell Technologies, Vancouver, Canada) according to manufacturer instructions, washed and prepared for flow cytometry phenotyping. GBM tumor samples were mechanically disrupted and digested in a mixture of DNAse I (Worthington Biochemical, LS002006, Lakewood, NJ) and Collagenase IV (Worthington Biochemical, LS004210, Lakewood, NJ). Following digestion, tumor samples were passed through 70 μm and 40 μm cell strainers to produce a single cell suspension. PBMCs were then isolated by Lymphoprep density gradient and cells were washed and prepared for flow cytometry phenotyping.

NK cells, harvested from GBM patient and healthy donor whole blood and tumor samples as described, were assessed via flow cytometry for NK cell surface receptor expression. Briefly, cells were washed twice and stained for surface ligands for 1 h in FACS buffer (1 x PBS supplemented with 2% FBS and 0.5 mM EDTA). Cells were washed and resuspended in FACS buffer containing Sytox Green (Thermo Fisher Scientific, Franklin Lakes, NJ) or Sytox Blue (Thermo Fisher Scientific, Waltham, MA), per manufacturer recommendations, prior to analysis on a BD Fortessa X-20.

Cell sorting and phenotyping

Antibodies used for flow cytometry and cell sorting were CD3-PeCy7 (BD, UCHT1, Franklin Lakes, NJ), CD56-PeCy5.5 (Thermo Fisher Scientific, CMSSB, Waltham, MA), TIGIT-APC (Biolegend, A15153G, San Diego, CA), DNAM-1-BV510 (Biolegend, 11A8, San Diego, CA), Sytox Green (Thermo Fisher Scientific, Franklin Lakes, NJ), Sytox Blue (Thermo Fisher Scientific, Waltham, MA), CD16-BUV395 (BD, 3G8, Franklin Lakes, NJ), NKG2A-FITC (Miltenyi Biotec, REA110, Gaithersburg, MD), CD158e1-BV421 (BD Biosciences, DX9, Franklin Lakes, NJ), PD-1-BV510 (Biolegend, NAT105, San Diego, CA), NKG2D-BV605 (Biolegend, 1D11, San Diego, CA), CD57-BV605 (Biolegend, QA17A04, San Diego, CA), CD69-BV650 (Biolegend, FN50, San Diego, CA), LAG-3-BV650 (Biolegend, 11C3C65, San Diego, CA), NKp30-BV711 (Biolegend, P30-15, San Diego, CA), TIM-3-BV711 (Biolegend, F38-2E2, San Diego, CA), A2AR-PE (R&D Systems, 599717, Minneapolis, MN), CD94-PE (Biolegend, DX22, San Diego, CA), CD158b-APC/Fire750 (Biolegend, DX27, San Diego, CA), 41BB-APC/Fire750 (Biolegend, 4B4-1, San Diego, CA), and KLRG1-APC (Biolegend, SA231A2, San Diego, CA), CD96-PE (Biolegend, NK92.39, San Diego, CA), NKp46-BV785 (Biolegend, 9E2, San Diego, CA), CD56-APC (Thermo Fisher Scientific, CMSSB, Waltham, MA), TIGIT-BV421 (Biolegend, A15153G), IFN-γ-PerCP-Cy5.5 (Biolegend, 4S.B3, San Diego, CA), CD107a-PE (Biolegend, H4A3, San Diego, CA), m4-1BB-APC (Thermo Fisher Scientific, 17B5, Waltham, MA), mCD16/32-BV421 (Biolegend, 93, San Diego, CA), mNK1.1-BV510 (Biolegend, PK136, San Diego, CA), mCD11b-BV605 (Biolegend, M1/70, San Diego, CA), mCD27-BV650 (Biolegend, LG.3A10, San Diego, CA), mCD3-BV711 (Biolegend, 145-2C11, San Diego, CA), mLAG-3-BV785 (Thermo Fisher Scientific, C9B7W, Waltham, MA), mTIGIT-PE-Cy7 (Biolegend, 1G9, San Diego, CA), mDNAM-1-APC-Fire 750 (Biolegend, 10E5, San Diego, CA), and mCD96-PE (Biolegend, 3.3, San Diego, CA). Samples were prepared as described and run on a BD Fortessa X-20 and analyzed using FlowJo V10. For sorting and TIGIT-subpopulation analysis live $CD56^{+}CD3^{-}$ were gated into three subpopulations: $TIGIT^{high}$ NK cells (MFI = 800–1200); $TIGIT^{medium}$ (MFI = 400–600); $TIGIT^{negative}$ (MFI = Isotype) using a BD FACS Aria (Sample histograms Figures S1 and S2). Sorted cells were allowed to rest for 48 h in RPMI media, supplemented with 10% FBS, 1% penicillin/streptomycin, and 500 IU rhIL-2 before use in functional assays. Throughout all analyses, NK cells were identified as NKp46+-$CD56^{+}CD3^{-}$due to high expression of CD56 on GBM target cells and GBM tumors.

Antibodies used in functional assays included anti-4-1BB (Thermo/Biolegend, 4B4-1, San Diego, CA and Waltham, MA), anti-4-1BB (Thermo, BBK-2, Waltham, MA), anti-TIGIT (Biolegend, A15153A, San Diego, CA), and anti-CD155 (Thermo Fisher Scientific, D171, Waltham, MA).

TCGA survival analysis

Survival analysis based on expression of individual queried genes or gene combinations (*TIGIT* and/or *PVR*) was done in GEPIA2 using TCGA gene expression data. Data were analyzed and generated using a Kaplan–Meier curve for overall survival (OS). Kaplan–Meier curves were generated with a median or quartile survival cutoff. The estimation of hazard ratios (HR) was done by Cox proportional hazards model regression analysis. A 95% confidence interval was set and used. Patient samples with expression level above the threshold were considered as the high-expression or high-risk cohort. cBioportal was used for gene co-expression analysis of *TIGIT* and *TNFRSF9* (4-1BB) based on the full RNA-seq V2 RSEM GBM PanCancer dataset (592 samples).

RNAseq analysis

Human NK cells were sorted as described, as $TIGIT^{high}$, $TIGIT^{medium}$ and $TIGIT^{negative}$, and total RNA was isolated using the mirVana miRNA Isolation Kit (Thermo Fisher Scientific, Waltham, MA) according to manufacturer instructions, with >700 ng of RNA per sample. All samples were checked for quality prior to analysis by Agilent Bioanalyzer, with DV200 > 80 and RIN >8.4 for all samples. Samples were sent to GeneWiz for library preparation and sequencing. Each sample contained at least 30 million paired-end reads with length of 250 bp. Data quality control (adapter trimming, minimum Phred score 30, minimum read length 50 bp) was performed using fastp[36] (version 0.19.5). Quality trimmed reads were mapped to human reference genome (GRCh38) using the STAR aligner[37] (version 2.7.9a). Reads aligned to each gene feature were counted using the featureCounts[38] program from Subread package (version 1.6.1). Differential expression (DE) analysis was performed using the edgeR method[39] (version 3.32.1) and genes with False Discovery Rate (FDR) ≤ 0.01 were denoted as significant.

Pathway analysis of RNAseq gene expression data

Functional and pathway enrichment analysis was performed using R-package clusterProfiler[35] (v3.18.1) and GSEA tool[40,41] (version 4). Gene enrichment set analysis (GSEA) was used to find pathways significantly enriched between $TIGIT^{high}$, $TIGIT^{medium}$, and $TIGIT^{negative}$ ($p < 0.05$). The Biocarta database was used for this analysis, and GSEA was performed on a pre-ranked gene list with (signed log2FC*-log10p value) used as the ranking criteria.

TIGIT-sorted NK cell phenotyping and function

For sorting and TIGIT-subpopulation analysis, live $CD56^{+}CD3^{-}$ NK cells were gated into three subpopulations: $TIGIT^{high}$ NK cells (MFI = 800–1200); $TIGIT^{medium}$ (MFI = 400–600); $TIGIT^{negative}$ (MFI = Isotype) (Sample histograms Figure S2). Sorted cells were allowed to rest for 48 h in RPMI media, supplemented with 10% FBS, 1% penicillin/streptomycin, and 500 IU rhIL-2 before use in functional assays. Killing was measured as described via LDH activity using the CytoScan LDH Assay Kit (G Bioscience) according to manufacturer instructions. For CD107a and IFN-γ expression analysis, NK cells were cocultured for 4 h with GBM43 WT cells in media containing CD107a-PE. Brefeldin A and monensin were added after 1 h of coculture. After 4 h NK cells were harvested, stained for CD56/CD3 surface markers, fixed, permeabilized, and stained for intracellular cytokines (IFN-γ), before being analyzed on the BD Fortessa (Figure S3).

For determination of glycolytic activity, sorted $TIGIT^{high}$/$TIGIT^{medium}$/$TIGIT^{negative}$ NK cells were cultured for 24 or 48 h and glycolysis was measured according to manufacturer instructions via the Glycolysis Cell-Based Assay kit (Cayman Chemical, Ann Arbor, MI).

Generation of CRISPR/Cas9 TIGIT knockout NK cells

TIGIT knockout NK cells were generated from purified NK cells, expanded for one week using K562 feeder cells as described, using the Human TIGIT Gene Knockout Kit v2 (Synthego, Redwood City, CA). Three sgRNA sequences were utilized, along with Cas9 protein to generate RNP complexes: 1) UCUUCCCUAGGAAUGAUGAC, 2) AUGUCACCUCUCCUCCACCA, and 3) GGCCAUUUGUAAUGCUGACU. 5×10^{6} NK cells were electroporated in OptiMEM medium in 100 μL in a 2 mm cuvette, with RNP complex, formed by incubating for 20 min 65 μg of True Cut HiFI Cas9 v2 (Thermo Fisher, A36498, Waltham, MA) with 5 μL of 100uM sgRNA, reconstituted in TE buffer, or TE buffer as a control, using the following conditions on a Biorad GenePulser 2.0 electroporation system: Square wave, 250 V, 4.0 ms pulse length, 5 pulses, 5s pulse interval. Following electroporation, NK cells were allowed to rest for 72 h, and then expanded for one week using K562 feeder cells as described prior to phenotype and functional assays.

NK cell phenotyping and cytokine screening on GBM co-culture

For phenotyping of NK cells and quantification of cytokine levels in response to GBM, sample groups consisted of NK cells alone, GBM43 cells alone, and NK cells co-incubated with GBM43 cells: without mAb blockade, with CD155 mAb (10 μg/mL), with TIGIT mAb (50 μg/mL), with both mAbs. GBM43 cells were seeded at 40,000 cells/well overnight. GBM43 and NK cells were preblocked with mAbs for 1 h prior to coincubation. NK cells were seeded at 100,000 cells/well, 1E6 cells/mL and coincubated for 24 h. NK cells were removed, GBM43 were trypsinized and collected for FACS phenotyping.

Cytokine secretion analysis was performed by Eve Technologies. Briefly, sample groups were cocultured as described above. Supernatant was taken and centrifuged at 300g for 10 min to remove NK cells, then at 3000g for 10 min to remove debris. Supernatant was sent to Eve Technologies for cytokine array analysis (Human Cytokine Array Proinflammatory Focused 15-plex).

For TIGIT KO phenotyping assays, WT or TIGIT KO NK cells were co-incubated for 24 h with GBM43-WT cells with or without TIGIT mAb (50 μg/mL). Expression of 4-1BB was measured via flow cytometry.

Enzyme-linked immunosorbent assay

NK cells were cocultured for 24 h GBM43 WT cells, with or without TIGIT mAb (50 μg/mL). Soluble CD16 was measured via human CD16a ELISA (Thermo Fisher Scientific, Waltham, MA) according to manufacturer instructions to assess if TIGIT blockade induces CD16 shedding.

CD155 knockdown in GBM

GBM43 cells were seeded at 200,000 cells/well in a 12 well and allowed to incubate overnight. The next day complete medium containing DMEM (- sodium pyruvate) +10% FBS +1% HEPES +5 μg/mL polybrene was added to cells and after 5 min, 10 μL CD155 shRNA lentiviral particles (50,000 IFU; Santa Cruz Biotechnology, Dallas, TX). After 24 h media was replace and after another 24 h cells were passaged 1:4. After 48 h cells were selected using 5 μg/mL puromycin dihydrochloride (Alfa Aesar, Haverhill, MA). Medium containing puromycin was changed every 3–4 days until resistant colonies were identified.

Cells were assayed for CD155 expression via flow cytometry (CD155-PE, Biolegend, SKII.4; Mouse IgG1-PE, Biolegend, MOPC-21, San Diego, CA) and analyzed on a BD Fortessa. For proliferation, GBM43-WT or CD155-KD cells were plated at 10,000 cells/well for 3 days. Proliferation was measured using CCK8 (ApexBio, Houston, TX) according to the manufacturer's instructions.

CD155 pharmacological inhibition assays

For cytotoxicity assays, NK cells were cocultured with GBM43-WT cells at E:T ratios of 2.5:1, 5:1, and 10:1 for 4 h, with or without TIGIT (50 μg/ML, Biolegend, A15153A, San Diego, CA) and/or CD155 (10 μg/mL, Thermo Fisher Scientific, D171, Waltham, MA) antibody blockade. Killing was measured via LDH activity using the CytoScan LDH Assay Kit (G Biosciences, St. Louis, MO) according to manufacturer instructions.

In vivo GBM CD155 KD studies and NK cell analysis

GBM43 WT and CD155-KD cells (3×10^6 cells/mouse) were subcutaneously (SC) inoculated into the left flank of RAG1$^{-/-}$ or NRG mice. Experimental groups consisted of PBS control mice, without any tumor (n = 4), GBM43 WT tumor bearing mice (n = 4), and GBM43 CD155-KD tumor bearing mice (n = 4). Tumor dimensions (L, W, H) and bodyweight measurements were monitored and the tumor volume was calculated according to the formula: $V = 0.52 \times L \times W \times H$. Tumor growth was monitored until mice met a predefined endpoint criteria. In some studies NK cells were depleted by administering anti-NK1.1 mAb (BioXCell, PK136, Lebanon, NH) one day prior to tumor inoculation and every 3 days until study endpoint. For RAG1$^{-/-}$ mice, whole blood and tumors were harvested from all mice. Serum samples were collected from whole blood, diluted 2-fold, and sent to Eve technologies for cytokine array analysis (Mouse Cytokine Array Focused 10-plex). Whole blood was collected via cardiac puncture and collected in K2EDTA Microtainers (BD, 365974, Franklin Lakes, NJ), and tumors were harvested. Tumor samples were minced digested by DNAse IV and Collagenase, as described, and red blood cells (RBCs) were removed from whole blood and tumor samples using ACK lysing buffer (Thermo Fisher, Waltham, MA). Samples were washed with FACS buffer and prepared for flow cytometric analysis as described. NK cells were isolated from whole blood and tumors and analyzed via flow cytometry. Additionally, circulating NK (cNK) cells were cultured overnight in RPMI containing 10% FBS, 1% P/S, and 500 IU/mL IL-2 and re-challenged in a GBM43 WT cytolysis assay at E:T ratios of 2.5:1, 5:1, and 10:1. GBM43 WT and CD155-KD tumor samples were additionally sent for histological (IHC) analysis.

Histological analysis

Immunohistochemical staining (IHC) was carried out at the Histology Research Laboratory at the Purdue University College of Veterinary Medicine. Briefly, tumors were fixed in 10% neutral-buffered formalin, embedded in paraffin, and cut into 3–5 μm sections.

For GBM43-WT and CD155-KD xenografts, mouse NK cells were detected through staining with NKp46/NCR1 (R&D Systems, AF2225, Minneapolis, MN) antibody, and NK activity was measured via Granzyme B (Abcam, ab4059, Waltham, MA) staining. IHC images were visualized using Aperio ImageScope software and manually quantified. For quantification of NK cells in tumors stained cells were counted in 4 randomly selected intratumoral fields of each slide at 200× magnification. Similarly, granzyme B$^+$ NK cells were quantified in 4 randomly selected intratumoral fields of each slide at 200× magnification. Quantification of NKp46$^+$ and granzyme B$^+$ cell counts between GBM43 WT and GBM43 KD groups were compared using an unpaired Student's *t* test.

4-1BB cytolysis assays

NK cells were cocultured with GBM43-WT cells, U87MG cells, or GBM10 cells at E:T ratios of 2.5:1, 5:1, and 10:1 for 4 h, with 4-1BB mAb (4B4-1 and BBK-2, 10 μg/mL), with or without TIGIT mAb (50 μg/mL) blockade. Killing was measured via LDH activity using the CytoScan LDH Assay Kit (G Biosciences, St. Louis, MO) according to manufacturer instructions.

In vivo 4-1BB/TIGIT targeting in GBM and tumor-infiltrating NK cell analysis

GBM43 WT cells (3×10^6 cells/mouse) were subcutaneously (SC) inoculated into the left flank of NRG mice. Experimental groups consisted of PBS control mice (n = 5), mice receiving NK cells (n = 5), mice receiving NK cells and TIGIT mAb (n = 5), mice receiving NK cells and 4-1BB agonistic mAb (4B4-1) (n = 5), and mice receiving NK cells, TIGIT mAb, and 4-1BB agonistic mAb (4B4-1) (n = 5). NK cells (5×10^6 cells/mouse) were administered i.v. weekly to all groups except the PBS control, with all groups receiving NK cells also receiving rhIL-15 i.p. twice weekly (0.5 μg/mouse). TIGIT mAb was administered i.p. (2 mg/kg) twice weekly, and 4-1BB mAb was administed i.p. (1 mg/kg) twice weekly. Tumor

dimensions (L, W, H) and bodyweight measurements were monitored and the tumor volume was calculated according to the formula: V = 0.52 × L × W × H. Tumor growth was monitored until mice met a predefined endpoint criteria. NK cells were isolated from whole blood and tumors and analyzed via flow cytometry for activating and inhibitory markers.

QUANTIFICATION AND STATISTICAL ANALYSIS

Prism 9 (Graphpad, Boston, MA) was used for statistical analysis with a $p < 0.05$ (*) considered significant. Ordinary one-way analysis-of-variance (ANOVA) tests along with Tukey's post-hoc test were used to compare multiple groups. two-way ANOVA tests along with Tukey's post-hoc test were used for comparison of treatment groups in mouse studies. Unpaired student t-tests were used for single-data comparisons of independent groups. Kaplan-meier statistical tests were used for comparison of survival groups in plots depicting TCGA survival data from GBM patients. Statistical parameters were calculated for correlative analyses using simple linear regression. Data are represented as mean ± SEM. *$p < 0.05$, **$p < 0.01$, ***$p < 0.001$, ****$p < 0.0001$.